NASA TM-81361

CORRELATION OF PREDICTED AND FLIGHT DERIVED STABILITY AND CONTROL DERIVATIVES - WITH PARTICULAR APPLICATION TO TAILLESS DELTA WING CONFIGURATIONS

Joseph Weil and Bruce G. Powers

July 1981

NASA

NASA TM-81361

CORRELATION OF PREDICTED AND FLIGHT DERIVED STABILITY AND CONTROL DERIVATIVES - WITH PARTICULAR APPLICATION TO TAILLESS DELTA WING CONFIGURATIONS

Joseph Weil and Bruce G. Powers
Dryden Flight Research Center
Edwards, Calif.

National Aeronautics and
Space Administration

1981

CORRELATION OF PREDICTED AND FLIGHT DERIVED STABILITY AND CONTROL DERIVATIVES - WITH PARTICULAR APPLICATION TO TAILLESS DELTA WING CONFIGURATIONS

Joseph Weil and Bruce G. Powers
Dryden Flight Research Center

INTRODUCTION

During the initial development of the space shuttle orbiter it was found that the flight control system performance was sensitive to uncertainties in a number of stability and control derivatives. Differences between predicted and flight experienced characteristics were of particular concern, inasmuch as the orbiter test program does not allow the flexibility of the incremental flight envelope buildup available to conventional airplanes.

The Dryden Flight Research Center had performed numerous investigations in which wind tunnel data were correlated with full scale flight test results and at the request of Johnson Space Center agreed to examine pertinent correlations to determine what maximum uncertainties might be encountered in the first shuttle entry from orbit - at least in the Mach range below 3, where the great majority of data existed.

Inasmuch as designers in the aerospace community might be able to apply the results of the correlations herein, it was decided to make the information originally assembled in 1976 available for general use.

SYMBOLS

ALT approach and landing test

C_{ℓ} rolling moment coefficient

$C_{\ell_{\beta}} = \partial C_{\ell} / \partial \beta$

$C_{\ell_{\delta_a}} = \partial C_{\ell} / \partial \delta_a$

$C_{\ell_{\delta_r}}$ $= \partial C_\ell / \partial \delta_r$

C_m pitching moment coefficient

$C_{m_{C_N}}$ $= \partial C_m / \partial C_N$

$C_{m_{\delta_e}}$ $= \partial C_m / \partial \delta_e$

C_N normal force coefficient

C_n yawing moment coefficient

C_{n_β} $= \partial C_n / \partial \beta$

$C_{n_{\delta_a}}$ $= \partial C_n / \partial \delta_a$

$C_{n_{\delta_r}}$ $= \partial C_n / \partial \delta_r$

C_Y lateral force coefficient

C_{Y_β} $= \partial C_Y / \partial \beta$

FLT flight

M Mach number

PRED predicted

q dynamic pressure

T. E. trailing edge

α angle of attack, deg

β sideslip angle, deg

Δ increment (flight predicted)

δ_a aileron deflection, $\frac{\delta_{e_L} - \delta_{e_R}}{2}$, deg

δ_e elevator deflection, $\frac{\delta_{e_L} + \delta_{e_R}}{2}$, deg

δ_r rudder deflection, deg

Λ wing sweep angle, deg

Subscripts:

L left

MAX maximum

R right

APPROACH

Task

The task consisted of the examination of all available and applicable flight versus predicted correlation data to determine a reasonable estimate of the extreme uncertainties from the nominal predicted derivative values. Nominal values as defined herein are derivatives obtained from rigid wind-tunnel tests corrected for aeroelasticity.

Applicable Configurations

The orbiter, with its thick double delta wing and large blunt fuselage, is a rather unusual vehicle (fig. 1). Furthermore, sources of good flight test versus predicted correlations are limited. Figure 2 presents a summary of the geometric characteristics sought and those possessed by the aircraft selected for inclusion in the analysis together with some clarifying remarks.

The desired geometric characteristics were a classic tailless delta design where trailing-edge wing flaps provide the required longitudinal and lateral control. The presence of a single vertical tail and a large fuselage relative to wingspan would also have been desirable. Unfortunately there was no single airplane that provided such geometry.

The XB-70 airplane (fig. 3) had the requisite wing flap controls but a relatively thin (2 to 2.5 percent thick) delta wing, a rather slender fuselage, twin vertical tails, and a canard.

The delta wing YF-12 airplane (fig. 4) had large engine nacelles at midspan and twin vertical tails.

The X-15 configuration (fig. 5) was dissimilar to the orbiter, but because it was one of the few sources of hypersonic data it could not be totally ignored.

Very limited data were used from the transonic aircraft technology (TACT) airplane (wing swept 58°) and from the British HP-115 programs.

The B-58 (fig. 6) and Concorde (fig. 7) airplanes had generally acceptable geometry and a good predictive base and Mach coverage.

The YF-16 and F-8 supercritical wing (SCW) airplanes were used only as a source of rudder control data.

The lifting bodies (figs. 8 and 9) had (by a stretch of the imagination) a delta planform as well as trailing edge longitudinal and lateral controls. However, it is believed that the flow phenomena were not similar to those for the orbiter, particularly in view of the multi-tailed aft body. The lifting bodies were considered a unique class of rather extremely shaped vehicles. Therefore the considerable store of information available for these shapes was judged to provide a measure of the extreme variations of flight and predicted characteristics that would not be exceeded by the orbiter; thus, the data were included.

Scope of Correlations

The specific parameters correlated in the investigation are noted in figure 10 for each of the applicable vehicles.

There were several reasons that certain data were not utilized in the studies. The XB-70, YF-12 and X-15 airplanes incorporated all-moving vertical tails, and hence rudder data were not available. The X-15 and TACT airplanes were equipped with slab horizontal tails for longitudinal and lateral control, so the aileron and elevator control derivatives were not considered meaningful. As mentioned previously, the YF-16 and F-8 SCW airplanes were included only to provide badly needed rudder effectiveness data.

In a few other instances data were not correlated because they were unavailable or because serious questions existed relative to quality. Although it is known that much effort was spent on Concorde wind-tunnel versus flight correlations, the

only data available to the authors were the limited results presented in reference 1.

The data used in this study were obtained from references 1 to 11 and from unpublished sources.

FACTORS AFFECTING CORRELATION CREDIBILITY

Inasmuch as the data used in this study were acquired from many sources and over a significant time span, it was felt that some means was required to assess the quality or credibility of the individual correlations. In order to accomplish this, the correlation credibility index shown in figure 11 was established.

Wind-Tunnel Test Factors

Model fidelity. - Because the bulk of wind-tunnel testing is usually done before a design is completely frozen, there may be important differences between the model and the full scale airplane. In such instances it is necessary to estimate the effects of the discrepancies.

Test coverage. - Although systematic wind-tunnel data are certainly easier to come by than similarly complete flight data, it is often impractical to obtain a sufficient matrix of data for newer configurations having many moving surfaces. Particular care must be taken to provide information near trimmed flight conditions. Of special importance is the availability of control effectiveness at small surface deflections and sideslip characteristics at small angles of sideslip.

Tunnel suitability. - This factor pertains to the general suitability of the wind-tunnel and model support system to the particular type of test being conducted. There are numerous instances of too large a model being used in a facility, particularly near sonic speed.

Measurement accuracy and scope. - Some of the items in this category are availability of accurate tare data and supplemental information such as pressure distributions, strain gage measurements, oil flow studies, and Schlieren pictures, which might enhance the basic force and moment data.

Flight Test Factors

Test coverage. - Optimum coverage would provide data at several Mach numbers over a reasonable angle-of-attack range with an emphasis on small increments in regions of rapid change. This permits spurious data points to be "faired out." It is also desirable, where feasible, to test at several altitudes with overlapping Mach numbers and angles of attack to provide a check on aeroelastic effects. Too often test coverage is sparse, which makes it difficult to provide a rational fairing of data points where nonlinearities may occur.

Data acquisition system. - Some of the earlier programs have suffered from inadequacies in the analog instrumentation systems - zero shifts, poor resolution, and nonoptimum scaling. Frequently, contractor sponsored programs have not had sufficient resources to maintain current calibration.

For situations where a high temperature environment is encountered, insensitivity to heat soak is required for pertinent instrumentation.

The inherent accuracy and adaptability of modern digital acquisition systems has the potential of fulfilling the requirements of most correlation programs.

Data analysis methods. - Prior to the period from 1965 to 1970, the Dryden Flight Research Center used several analog methods to derive stability and control derivatives from flight maneuvers. Although the results were usually reasonably acceptable, the techniques left much to be desired. In the 1960's Dryden developed a versatile method for determining derivatives that had many advantages and is now accepted internationally. A good discussion of this preferred method (referred to as the modified maximum likelihood estimator, or MMLE) can be found in references 12 and 13.

Mass and inertia accuracy. - Accurate knowledge of weight, the moments of inertia, and the principal axis inclination are required. Moments of inertia and principal axis inclination are usually calculated by the weight and balance department of the manufacturer. Where possible, experimental checks obtained by "swinging the airplane" improves confidence in these values (ref. 14).

Other Considerations

Matching test conditions. - This factor assesses how well the flight and wind-tunnel test conditions match. The test conditions include Mach number, leading and trailing edge flap settings, speed brake deflection, and so forth. In the most serious correlation efforts the wind-tunnel tests are performed after the flight tests to insure maximum compliance.

Basis for full-scale extrapolations. - Wind-tunnel data are almost always obtained with essentially rigid models, whereas the full scale airplane can experience significant aeroelastic effects in the higher dynamic pressure regimes that can drastically affect correlation. Accurate aeroelastic corrections are not always readily available, and the analytical base must be carefully examined, particularly where large corrections are predicted.

Another factor in this category is the derivation of any Reynolds number correction that may be required.

Experience and motivation of correlators. - This last factor, namely, the experience and motivation of the individual responsible for a particular correlation effort, is certainly one of the most important elements. In fact, the better efforts usually involve representatives of both the flight test and wind-tunnel disciplines as active members of the test team to achieve the required depth of background.

Correlation Credibility Index

The index in figure 11 has not been applied to each of the separate correlations that were used in this paper. However, it does allow us to make some general categorizations of the data used.

There were relatively few truly high quality "A" rating correlations, and they will be referred to later in the discussion. In all cases a major effort was required to achieve the excellence attained. This generally involved fabrication of a carefully scaled model of the actual airplane flown, with the wind-tunnel testing of the model accomplished after the flight tests were completed. Correlation was the primary program objective.

Most of the data used would fall in the "B" rating category. Reasonable care was exercised in the conduct of the

overall effort, but flight-to-wind-tunnel correlation was but one of four or five major program objectives. The NASA/Air Force Flight Test Center (AFFTC) lifting-body investigation would be assigned this designation.

Several programs exhibited definite shortcomings that would require certain elements to be rated marginal at best. These will be identified where appropriate.

METHOD OF ANALYSIS

Typical Procedure

The M2-F3 results will be used to illustrate the procedure followed in analyzing the flight derivative data. The angle-of-attack/Mach number envelope over which flight derivatives were obtained is shown in figure 12. The nominal angle of attack was somewhat arbitrary but was close to a 1g value for the altitude profile used in the testing. It was decided to concentrate the analysis in a ±5° angle-of-attack range about the nominal value. A typical crossplot of a derivative (C_{n_β}) showing the variation with angle of attack is presented in figure 13 for a Mach number of approximately 1.1. Note that there is a small variation in Mach number with angle of attack (figs. 12 and 13) and that care must be exercised to limit this variation in regions of rapidly changing characteristics. The data points shown allow a reasonable fairing, with a single point clearly out of line. The predicted line was rigid wind-tunnel data. In this instance no correction was required for aeroelastic effects because of the rigidity built into the research airplane. The maximum deviation between flight and predicted results was 0.0006 for C_{n_β} at M = 1.1.

Format of Correlated Parameters

For many derivatives, a percentage deviation from the predicted value seemed to provide a logical correlating base that would not be affected by wing reference geometry. Thus the ratio of $\frac{\text{FLT - PRED}}{\text{PRED}}$ was used for correlating the primary control power parameters $C_{\ell_{\delta_a}}$, $C_{n_{\delta_r}}$, and $C_{m_{\delta_e}}$, as well as for $C_{\ell_{\delta_r}}$ and C_{Y_β}. For other parameters, such as $C_{n_{\delta_a}}$, C_{n_β}, and C_{ℓ_β},

where the predicted value might be near zero at times, the data were correlated in terms of FLT - PRED. This quantity is more sensitive to wing reference geometry, but the impact should be relatively minor for the data used in the present study, inasmuch as the wing geometry used for the aforementioned correlation parameters was generally similar. Other comments on this subject will be included in the discussion of results.

DISCUSSION OF BASIC CORRELATIONS

Lateral-Directional Parameters

$C_{n_{\delta_a}}$. - Flight measured $C_{n_{\delta_a}}$ has always been one of the most difficult parameters to correlate with wind-tunnel predictions. Moreover, experience has shown that $C_{n_{\delta_a}}$ can drastically affect lateral controllability, and therefore the ability to predict that particular derivative is often of considerable importance. The correlation of flight and predicted $C_{n_{\delta_a}}$ is presented in figure 14 for conventional airplanes and in figure 15 for lifting bodies. Note that aileron derivatives are based on average aileron deflection rather than total aileron deflection.

For the conventional aircraft the largest discrepancy occurred at Mach 0.95 and was in a negative direction. Above Mach 1.5 there is definite evidence of a decrease in the magnitude of the difference between flight values and predictions. At Mach numbers greater than 2.0 only B-70 and YF-12 data were available and the correlations were very good.

It should be noted that particular pains were taken to verify the maximum deviations for the B-70 at Mach 0.95, which included supplemental wind-tunnel tests.

The lifting body data (fig. 15) encompass a smaller Mach number range than was available for the conventional airplanes. With the exception of the extreme positive points for the HL-10 correlation at Mach numbers of 1.2 and 1.5, the maximum flight determined $C_{n_{\delta_a}}$ is more negative than predicted.

All of the data were considered in the formulation of reasonable maximum uncertainty limits. Below Mach 0.7 a value of ±0.0004 was selected. At transonic speeds the maximum uncertainty level was increased to ±0.0008. Above Mach 1.5 it appeared

appropriate to reduce the uncertainty as shown, although the data on which the supersonic boundaries are based are admittedly meager. Note that the uncertainty limits shown are based on engineering judgment rather than on a statistical weighting of the points.

$C_{\ell_{\delta_a}}$. - The correlations of the aileron effectiveness derivative, $C_{\ell_{\delta_a}}$, are presented in figures 16 and 17 for conventional aircraft and lifting bodies, respectively. There appears to be little variation with Mach number. For both sets of data the flight determined derivative showed more extreme values in the higher-than-predicted direction. Maximum uncertainty limits of 40 percent and -25 percent of the predicted values appeared to be reasonable choices. The higher value would be used for system limit cycle checks, and the lower value to determine adequate system gain to avoid stability problems.

$C_{n_{\delta_r}}$. - The correlation of the rudder effectiveness derivative $C_{n_{\delta_r}}$ is presented in figure 18 for conventional aircraft and in figure 19 for lifting bodies. Considerably more data were available from the lifting body programs than for the more conventional airplanes, and the lifting body data showed greater differences from the predicted results. Levels of 50 percent greater than predicted and 25 percent less than predicted are felt to represent reasonable maximum uncertainty values.

It is evident that the Concorde data fall outside the selected limits at low supersonic speed (fig. 18). However, the resolution of the plot from which the information was derived (ref. 1) was very low. Furthermore, the aeroelastic correction applied was at times greater than 60 percent of the rigid wind-tunnel data. Thus, it is likely that a good measure of the discrepancy is of aeroelastic rather than aerodynamic origin.

$C_{\ell_{\delta_r}}$. - The correlation of the rolling moment due to rudder deflection parameter, $C_{\ell_{\delta_r}}$, is presented in figures 20 and 21. Data were very limited for conventional airplanes, and the lifting body information was needed to determine maximum uncertainty limits. The limit values selected were 60 percent uncertainty

in the more-effective-than-predicted direction and 30 percent uncertainty in the less-effective-than-predicted direction. The fact that these limits were slightly greater than those proposed for $C_{n_{\delta_r}}$ may be due in part to the greater difficulty of measuring accurate values for $C_{\ell_{\delta_r}}$.

C_{n_β}. - A correlation of the directional stability parameter C_{n_β} is presented in figure 22 for conventional aircraft and in figure 23 for lifting bodies. For the conventional aircraft it would appear that somewhat greater discrepancies between flight measured and wind-tunnel C_{n_β} are indicated near Mach 1, with most of the flight values showing greater stability than predicted. At Mach numbers above 1.5 a maximum discrepancy of 0.0005 is indicated, with the flight values generally less than predicted.

The lifting body data fall mostly between Mach 0.6 and Mach 1.5 (fig. 23). For these configurations, unlike the conventional airplanes, there is a pronounced tendency for decreased flight stability relative to predictions, with the value of FLT - PRED as large as -0.0016 to -0.0017.

A conservative approach was followed in formulating the recommended limits at transonic speed, with a possible -0.0014 in the decreased stability direction and 0.0009 in the increased stability direction.

C_{ℓ_β}. - The rolling moment due to sideslip derivative, C_{ℓ_β}, correlated for conventional airplanes and lifting bodies in figures 24 and 25, respectively. Note the very good correlation for the X-15 at hypersonic speeds. The recommended uncertainty limits were ±0.0005 at subsonic speeds, ±0.0008 at transonic speeds and ±0.0003 above Mach 1.6.

C_{Y_β}. - The lateral force coefficient, C_{Y_β}, is correlated for conventional aircraft in figure 26 and for lifting bodies in figure 27. Most of the points fall within a ±25 percent band.

Longitudinal Parameters

$\delta_{e_{TRIM}}$. - As mentioned earlier, there are relatively few high quality thoroughly coordinated wind-tunnel-to-flight correlations. One effort worthy of note was made for the XB-70-1 airplane.

A program was undertaken by NASA to evaluate the accuracy of a method for predicting the aerodynamic characteristics of large supersonic cruise airplanes. This program compared predicted and flight measured lift, drag, angle of attack, and control surface deflection for the XB-70-1 airplane for 14 flight conditions with a Mach number range from 0.76 to 2.56. The predictions were derived from the wind-tunnel test data for a 0.03-scale model of the XB-70-1 airplane that was fabricated to closely represent the aeroelastically deformed shape at a Mach 2.5 cruise condition. Corrections for shape variations at the other Mach numbers were included in the prediction. The results of the study were described in references 3 and 4.

A correlation of flight and predicted trim δ_e is shown in figure 28 for the XB-70-1, YF-12, and two lifting body configurations. If the XB-70-1 point at Mach 1.06 that was derived from interpolated wind-tunnel data is disregarded, lines of ±4° variation bound all of the points except one.

ΔC_m. - Inasmuch as the trim surfaces of the aircraft used in figure 28 were of different size, it would appear that pitching moment coefficient uncertainties (ΔC_m) would provide a better correlation parameter than elevator deflection. Therefore the data in figure 28 were transformed into an equivalent ΔC_m using an appropriate value of $C_{m_{\delta_e}}$.

The lifting body data were originally reduced to coefficient form by using body length as the reference chord instead of the normal practice of using the mean aerodynamic chord (MAC). Accordingly, an MAC was calculated for each lifting body, and the elevator effectiveness was increased by the ratio of body length to MAC.

The results of the correlation of flight and predicted ΔC_m are presented in figure 29. There is a fairly rapid decrease in ΔC_m above Mach 1 due to the expected reduction in $C_{m_{\delta_e}}$. If the Mach 1.06 XB-70 point is disregarded, the HL-10 lifting body exhibits the largest change in ΔC_m from subsonic speed to Mach 1.6,

having a magnitude 2 to 3 times that for the other three aircraft shown. It is felt that the proposed limit shown (ΔC_m = 0.022 up to Mach 1.1, decreasing to a value of ΔC_m = 0.005 above Mach 1.8) is a reasonable and conservative maximum uncertainty guideline.

$C_{m_{\delta_e}}$. - A correlation of flight and predicted $C_{m_{\delta_e}}$ is shown in figure 30 for conventional aircraft and in figure 31 for lifting bodies. Most of the very sparse conventional airplane data are from the XB-70 data base. Much better coverage was available from the lifting bodies, and these latter data were used to arrive at the recommended uncertainty criteria of 40 percent over prediction and 20 percent less than prediction.

$C_{m_{C_N}}$. - A comparison of predicted and flight derived C_m variation with C_N is shown in figure 32. The overall stability in flight is considerably greater than predicted. However, there are very large differences in local slope due to the presence of nonlinearities. These nonlinear tendencies are often found in C_m data of low aspect ratio swept wing configurations, and for that reason it was decided not to specify a longitudinal stability uncertainty value.

APPLICATION OF RESULTS

As mentioned earlier, the prime motivation for the correlations presented in figures 14 to 31 was to provide a frame of reference that would be useful when assessing the critical aerodynamic uncertainties that would be required to produce either unacceptable flight control characteristics or total loss of control during the orbiter entry.

Probability of Exceeding Derivative Uncertainty Boundaries

Single uncertainties. - An examination of the data in figures 14 to 31 for a number of aerospace configurations in the transonic and low supersonic Mach number range led to the conclusion that the probability of occurrence of a single uncertainty of the magnitude specified by the boundaries might be as high as 10^{-2}. In most instances the chance of encountering such a magnitude deviation would be considerably more remote than 10^{-2}, but for the purposes of this study the greater probability was assumed.

Uncertainty pairs. - If a single uncertainty has an occurrence probability of 10^{-2}, it follows that the simultaneous occurrence of two derivative uncertainties would have a probability of 10^{-4}, assuming no aerodynamic interaction between the two derivatives.

In the case of the rudder parameters $C_{\ell_{\delta_r}}$ and $C_{n_{\delta_r}}$, one might assume an almost complete interdependence. In order to determine the actual degree of cross-correlation, the two parameters were compared for a series of lifting body configurations (fig. 33). If the coefficient of correlation was near unity, all of the points would fall along a 45° line. However, quite a bit of scatter is in evidence. For sensitivity studies it is recommended that when extreme uncertainties are being studied in either $C_{n_{\delta_r}}$ or $C_{\ell_{\delta_r}}$, the other parameter be maintained at zero uncertainty.

Uncertainty sets. - The overall lateral-directional behavior is affected by more than a score of individual derivatives. The probability of all of these derivatives simultaneously experiencing a limiting uncertainty in a degrading direction would be truly infinitesimal. However, the basic flight behavior of an airplane can be shown to be primarily a function of a handful of the most significant terms. If a value of 50 percent of the nominal uncertainty is applied to the four most significant terms of each set, the estimated probability of occurrence is about 10^{-4}.

Criteria for Flight Control System Capability in Degraded Aero-Situations

Based on flight test experience of highly augmented aircraft and intuitive reasoning, the following criteria were adopted. The flight control system (FCS) shall be able to cope with situations having an occurrence of probability greater than 10^{-4}. Thus (assuming a Gaussian distribution of the uncertainties) the FCS should be able to provide acceptable characteristics with:

(a) Any single derivative at 1.6 times the nominal uncertainty.

(b) Any two derivatives at the nominal uncertainty value.

(c) Sets with 0.5 of the nominal uncertainty applied to all terms.

Shuttle Orbiter Estimates

It is beyond the scope and purpose of this report to present in-depth results of the orbiter entry flight control characteristics with degraded aerodynamics. However, a brief summary of the study will indicate how the derivative uncertainties described here were applied to flight test planning for a particular program.

Single derivative uncertainties. - The single derivative uncertainties were evaluated by making simulated entries in the auto mode with progressively increasing values of the uncertainty. The most significant single uncertainty was a reduction in $C_{\ell_{\delta_a}}$. However, in order to achieve a significant degradation in control characteristics, an uncertainty factor of between 2 and 3 times nominal was required, which is about 50 percent above the assumed criteria boundary of 1.6 times nominal and is estimated to have a probability of occurrence of about 10^{-7}.

Uncertainty pairs. - In studying the uncertainty pairs a progressively increasing factor was applied to both terms in the pair. As might be expected, the most critical pairs included the $C_{\ell_{\delta_a}}$ uncertainty, which was the most critical single factor. All of the critical uncertainty factors were well above the DFRC criteria value of 1.0. The critical uncertainties were approximately twice the nominal uncertainties, and the probability of occurrence was estimated to be about 10^{-14}.

Uncertainty sets. - Based on engineering judgment and simplified analytical techniques a series of lateral-directional uncertainty sets was formulated. The same increasing uncertainty factor was applied to all terms in the set until a critical degradation in control was observed. All of the uncertainty sets had critical factors well above the criteria value of 0.5. The loss of control boundaries were all above a value of 1.0. A divergent loss of control occurrence would correspond to a probability of occurrence of about 10^{-13}.

Comparison of Orbiter Subsonic Derivative Uncertainties With Maximum Variation Criteria

The derivative data obtained during the subsonic approach and landing (ALT) tests (ref. 15) were assessed in terms of the predicted derivatives and then compared to the maximum uncertainties criteria shown in figures 14 to 31. The results are presented in figure 34 and indicate much better agreement between

flight and predicted results than have been observed in previous programs. Note, however, that the test envelope investigated was below the transonic Mach regime, where some of the largest differences are often experienced. Because of the quality and quantity of orbiter wind-tunnel data and the care exercised in analyzing the flight data an "A" rating in the correlation credibility index would appear warranted.

CONCLUDING REMARKS

Flight test and predicted derivatives for many airplanes have been correlated over a wide Mach number range. The results of the study would appear to offer a valuable source of standard uncertainties with which to test the sensitivity of modern command control systems, particularly for tailless delta wing configurations.

Dryden Flight Research Center
National Aeronautics and Space Administration
Edwards, California 93523
June 8, 1981

REFERENCES

1. Pelagatti, C.; Pilon, J. C.; and Bardaud, J.: Analyse Critique des Comparaisons des Resultats de Vol aux Previsions de Soufflerie Pour des Avions de Transport Subsonique et Supersonique. AGARD CP-187, Flight/Ground Testing Facilities Correlation, April 1976, pp. 23-1 -- 23-24.

2. Wolowicz, Chester H.; Strutz, Larry W.; Gilyard, Glenn B.; and Matheny, Neil W.: Preliminary Flight Evaluation of the Stability and Control Derivatives and Dynamic Characteristics of the Unaugmented XB-70-1 Airplane Including Comparisons With Predictions. NASA TN D-4578, 1968.

3. Wolowicz, Chester H.; and Yancey, Roxanah B.: Comparison of Predictions of the XB-70-1 Longitudinal Stability and Control Derivatives With Flight Results for Six Flight Conditions. NASA TM X-2881, 1973.

4. Arnaiz, Henry H.; Peterson, John B., Jr.; and Daugherty, James C.: Wind-Tunnel/Flight Correlation Study of Aerodynamic Characteristics of a Large Flexible Supersonic Cruise Airplane (XB-70-1). III - A Comparison Between Characteristics Predicted From Wind-Tunnel Measurements and Those Measured in Flight. NASA TP-1516, 1980.

5. Yancey, Roxanah B.: Flight Measurements of Stability and Control Derivatives of the X-15 Research Airplane to a Mach Number of 6.02 and an Angle of Attack of 25°. NASA TN D-2532, 1964.

6. Matheny, Neil W.; and Gatlin, Donald H.: Flight Evaluation of the Transonic Stability and Control Characteristics of an Airplane Incorporating a Supercritical Wing. NASA TP-1167, 1978.

7. Strutz, Larry W.: Flight-Determined Derivatives and Dynamic Characteristics for the HL-10 Lifting Body Vehicle at Subsonic and Transonic Mach Numbers. NASA TN D-6934, 1972.

8. Sim, Alex G.: Results of a Feasibility Study Using the Newton-Raphson Digital Computer Program To Identify Lifting Body Derivatives From Flight Data. NASA TM X-56017, 1973.

9. Sim, Alex G.: Flight-Determined Stability and Control Characteristics of the M2-F3 Lifting Body Vehicle. NASA TN D-7511, 1973.

10. Kirsten, Paul W.: Wind Tunnel and Flight Test Stability and Control Derivatives for the X-24A Lifting Body. FTC-TD-71-7, Air Force Flight Test Center, Edwards AFB, April 1972.

11. Nagy, Christopher J.; and Kirsten, Paul W.: Handling Qualities and Stability Derivatives of the X-24B Research Aircraft. AFFTC-TR-76-8, Air Force Flight Test Center, Edwards AFB, March 1976.

12. Iliff, Kenneth W.: Estimation of Aerodynamic Characteristics From Dynamic Flight Test Data. Dynamic Stability Parameters, AGARD-CP-235, Nov. 1978.

13. Maine, Richard E.; and Iliff, Kenneth W.: User's Manual for MMLE3, a General FORTRAN Program for Maximum Likelihood Parameter Estimation. NASA TP-1563, 1980.

14. Boucher, Robert W.; Rich, Drexel A.; Crane, Harold L.; and Matheny, Cloyce E.: A Method for Measuring the Product of Inertia and the Inclination of the Principal Longitudinal Axis of Inertia of an Airplane. NACA TN 3084, 1954.

15. Hoey, Robert G., et al.: AFFTC Evaluation of the Space Shuttle Orbiter and Carrier Aircraft - NASA Approach and Landing Test. AFFTC-TR-78-14, Air Force Flight Test Center, Edwards AFB, May 1978.

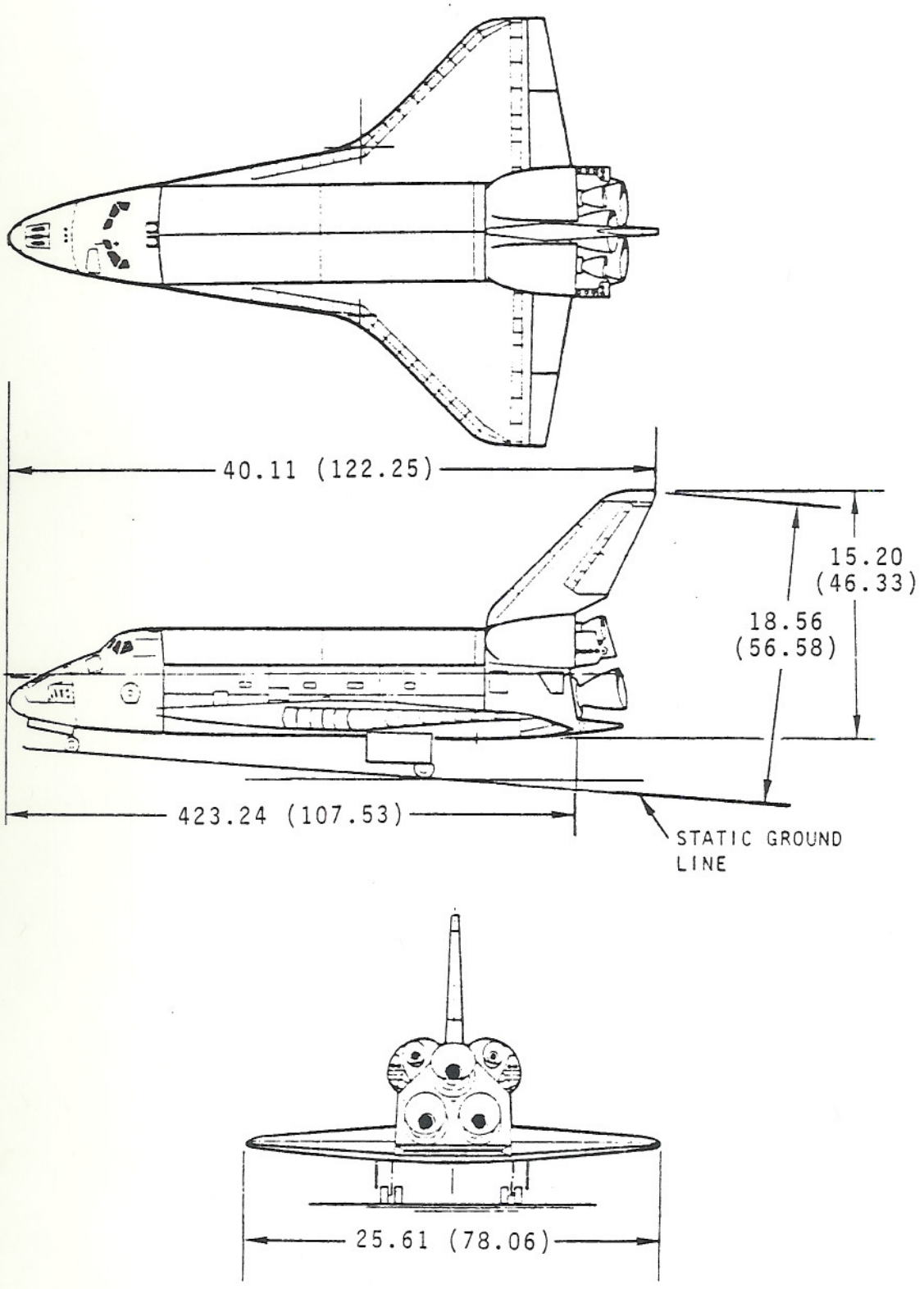

Figure 1. Three-view drawing of the orbiter. Dimensions are in meters (feet).

AIRCRAFT	GEOMETRIC FACTORS					REMARKS
	Δ WING PLANFORM	WING FLAP LONG. CONTROL	WING ELEVON LAT. CONTROL	SINGLE VERT. TAIL	LARGE FUS.	
XB-70	✓	✓	✓			GOOD PRED. BASE, M RANGE CANARD, LIMITED α RANGE
YF-12	✓	✓	✓			GOOD M RANGE, LIMITED α RANGE
X-15				✓	✓	WIDE α , M RANGE
TACT $\Lambda=58^{o}$	✓			✓	✓	ONLY LIMITED DATA CURRENTLY AVAILABLE
HP-115	✓	✓	✓	✓		LOW SPEED DATA ONLY
B-58	✓	✓	✓	✓		GOOD PREDICTIVE BASE, M RANGE
YF-16 F-8 SCW				✓		SOURCE OF RUDDER CONTROL DATA
LIFTING BODIES	✓	✓	✓			UNIQUE CLASS OF VEHICLE, LOW q OPERATION. GOOD α, M RANGE
CONCORDE	✓	✓	✓	✓		GOOD PREDICTIVE BASE, M RANGE ONLY LIMITED DATA AVAILABLE

Figure 2. Correlation applicability.

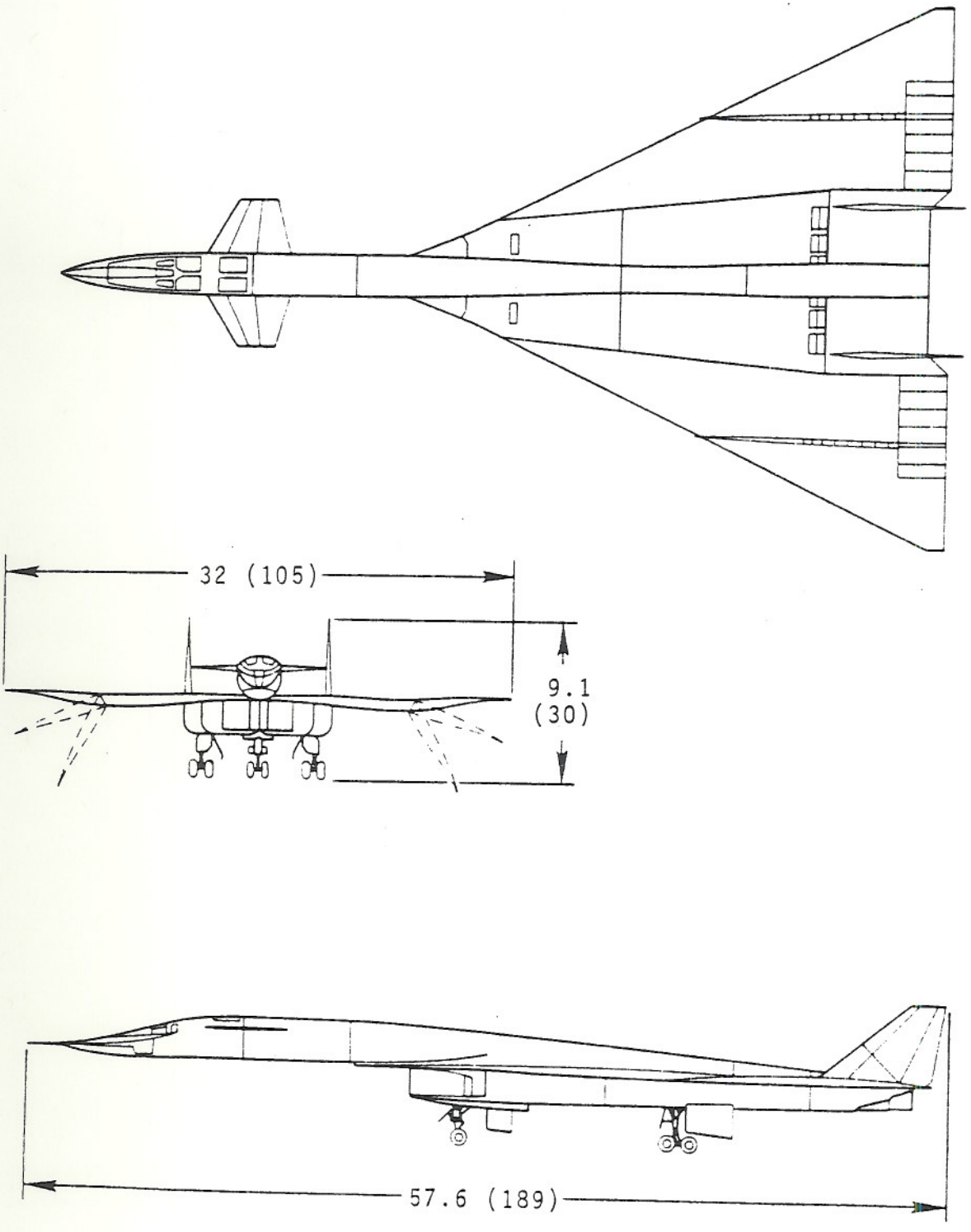

Figure 3. Three-view drawing of XB-70-1 airplane. Dimensions are in meters (feet).

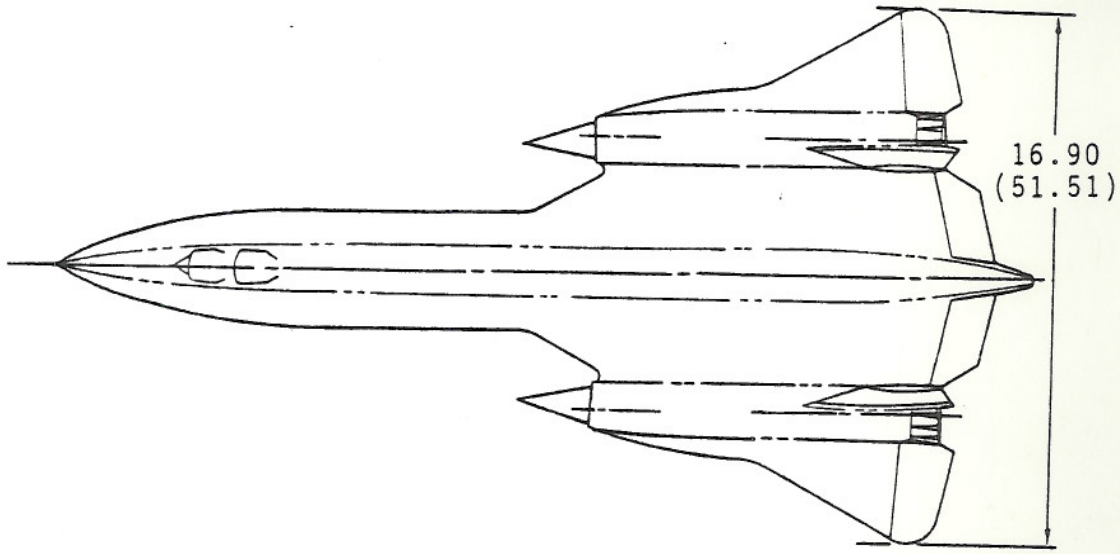

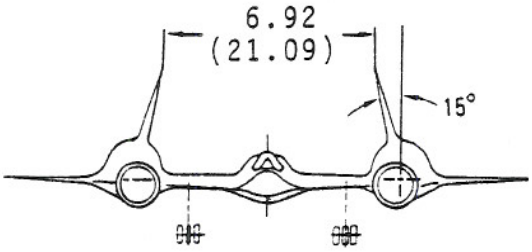

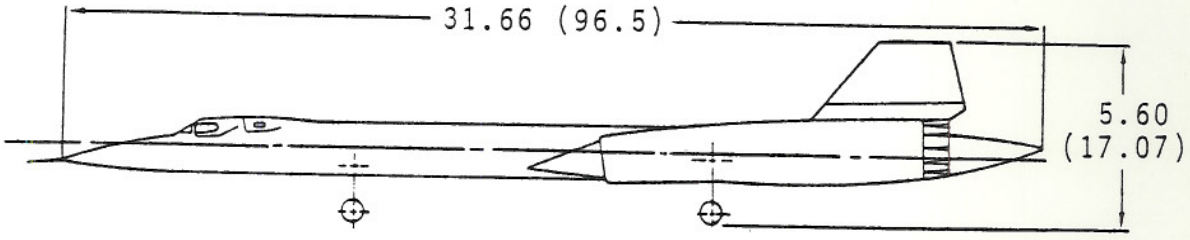

Figure 4. Three-view drawing of YF-12 airplane. Dimensions are in meters (feet).

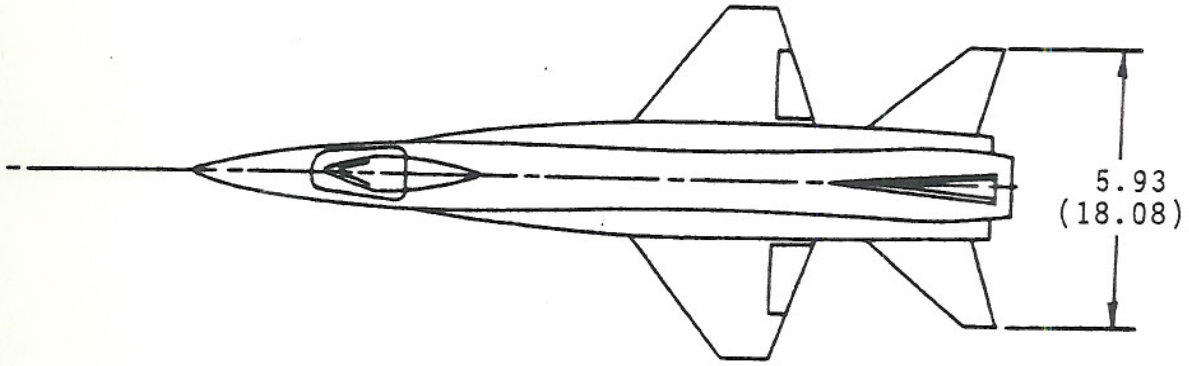

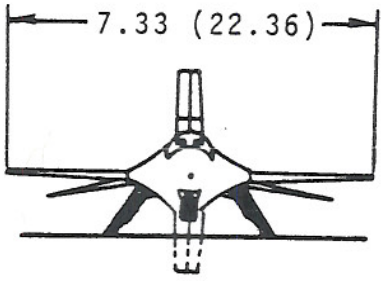

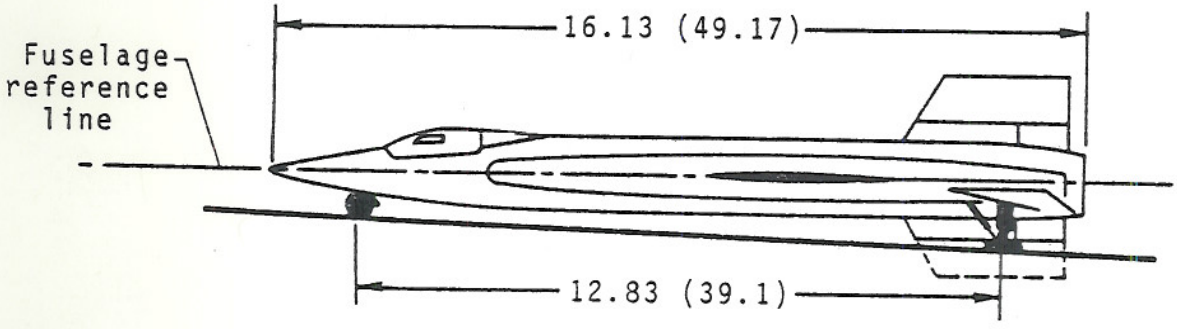

Figure 5. Three-view drawing of X-15 airplane. Dimensions are in meters (feet).

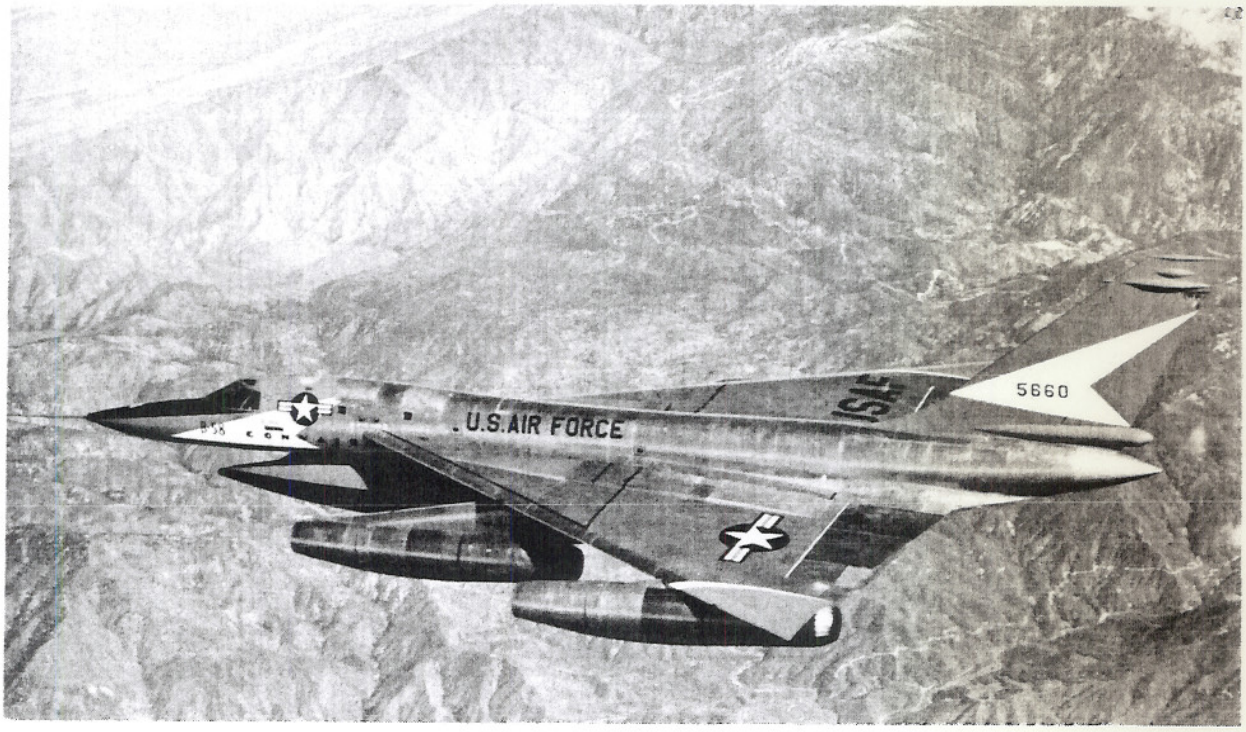

Figure 6. B-58 airplane.

Figure 7. Concorde airplane.

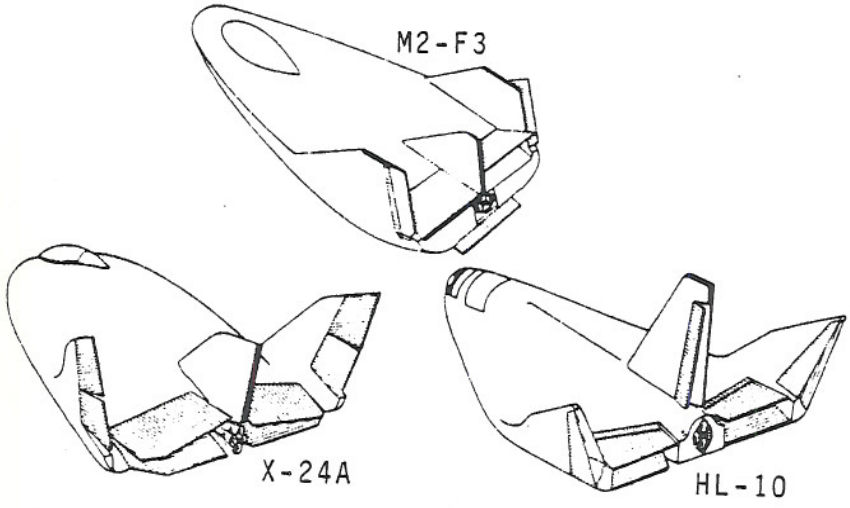

Figure 8. Sketch of M2-F3, HL-10, and X-24A lifting bodies showing control surfaces.

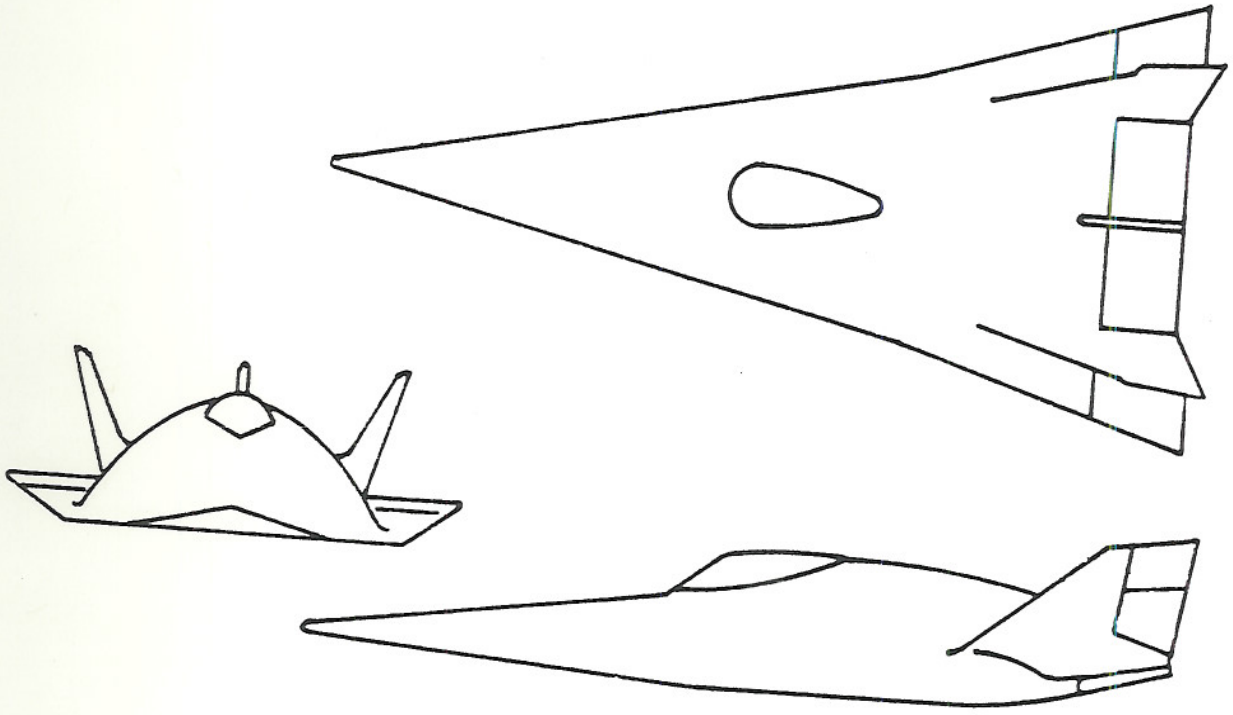

Figure 9. Three-view drawing of X-24B lifting body.

AIRCRAFT		PARAMETERS CORRELATED								
		$C_{n_{\beta_a}}$	$C_{\ell_{\beta_a}}$	$C_{n_{\delta_r}}$	C_{n_β}	C_{ℓ_β}	C_{Y_β}	$C_{m_{\delta_e}}$	TRIM	$C_{\ell_{\delta_r}}$
CONVENTIONAL	XB-70	✓	✓		✓	✓	✓	✓	✓	
	YF-12	✓	✓		✓	✓		✓	✓	
	X-15				✓	✓	✓			
	TACT*			✓	✓	✓				
	CONCORDE			✓	✓			✓		
	HP-115	✓	✓	✓	✓	✓	✓			
	B-58	✓	✓	✓	✓	✓				✓
	YF-16			✓						✓
	F-8 SCW			✓						✓
LIFTING BODIES	HL-10	✓	✓	✓	✓	✓	✓	✓	✓	✓
	M2-F3	✓	✓	✓	✓	✓	✓	✓	✓	✓
	X-24A	✓	✓	✓	✓	✓	✓	✓		✓
	X-24B	✓	✓	✓	✓	✓	✓	✓		✓

* Λ=58°

Figure 10. Correlation scope.

FLIGHT TEST FACTORS				WIND-TUNNEL FACTORS				GENERAL CONSIDERATIONS				
TEST COVERAGE	DATA ACQUISITION SYSTEM	DATA ANALYSIS METHODS	MASS AND INERTIA ACCURACY	MODEL FIDELITY	TEST COVERAGE	TUNNEL SUITABILITY	MEASUREMENTS ACCURACY AND SCOPE	MATCHING TEST CONDITIONS	INTER-CENTER COOPERATION	EXPERIENCE OF CORRELATORS	BASIS FOR FULL-SCALE EXTRAPOLATIONS	

RATING SYSTEM: EXCEPTIONAL (++), ABOVE AV. (+), SATISFACTORY (S), MARGINAL (-), DEFICIENT (--)

INDEX		RATING RATIONALE
A HIGH QUALITY CONTROL	1	(++) IN SEVERAL FACTORS, (+) IN REMAINING
	2	(+) IN MOST FACTORS, (S) IN ONE OR TWO
	3	MORE (+) THAN (S)
B REASONABLE CARE	1	MOST FACTORS (S) BUT SOME (+)
	2	MOST FACTORS (S) OR BETTER BUT ONE (-)
	3	(-) IN SEVERAL FACTORS
C MAJOR DEFICIENCY	1	(--) IN A SINGLE FACTOR OR (-) IN SEVERAL
	2	(--) IN TWO ELEMENTS
	3	(--) IN MOST FACTORS

Figure 11. Correlation credibility index.

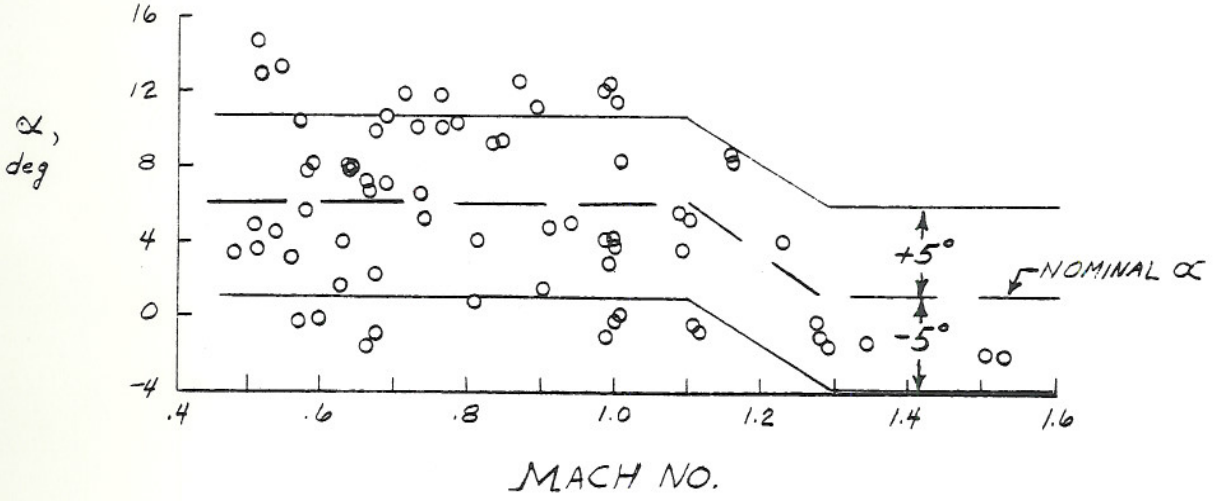

Figure 12. M2-F3 envelope.

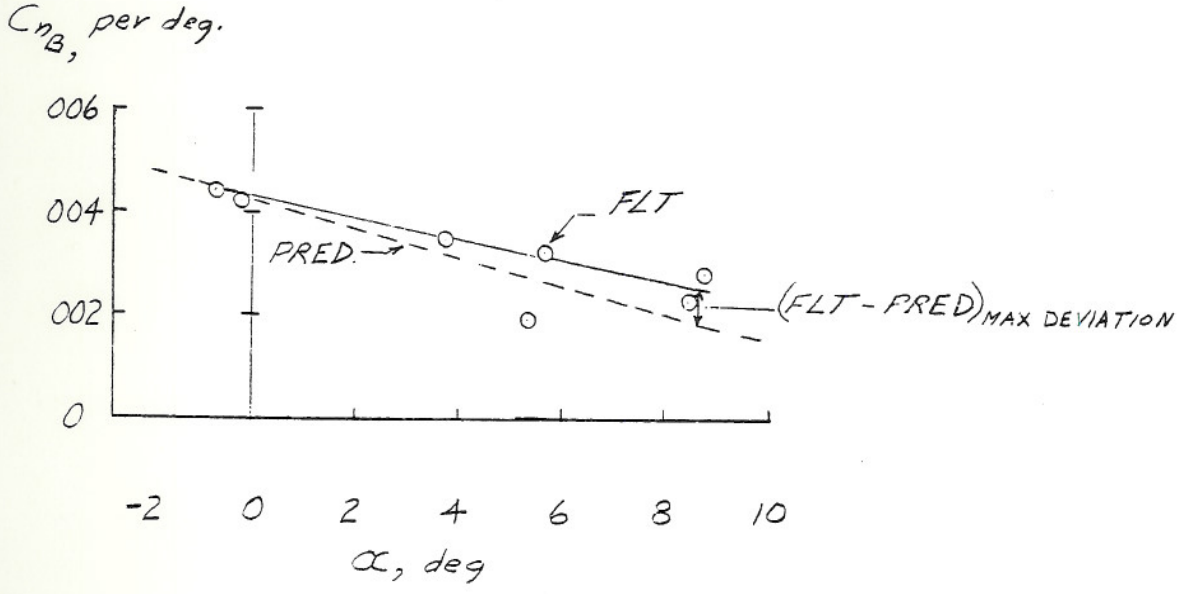

Figure 13. Typical basic data used for correlation summary. M2-F3; M ≈ 1.1.

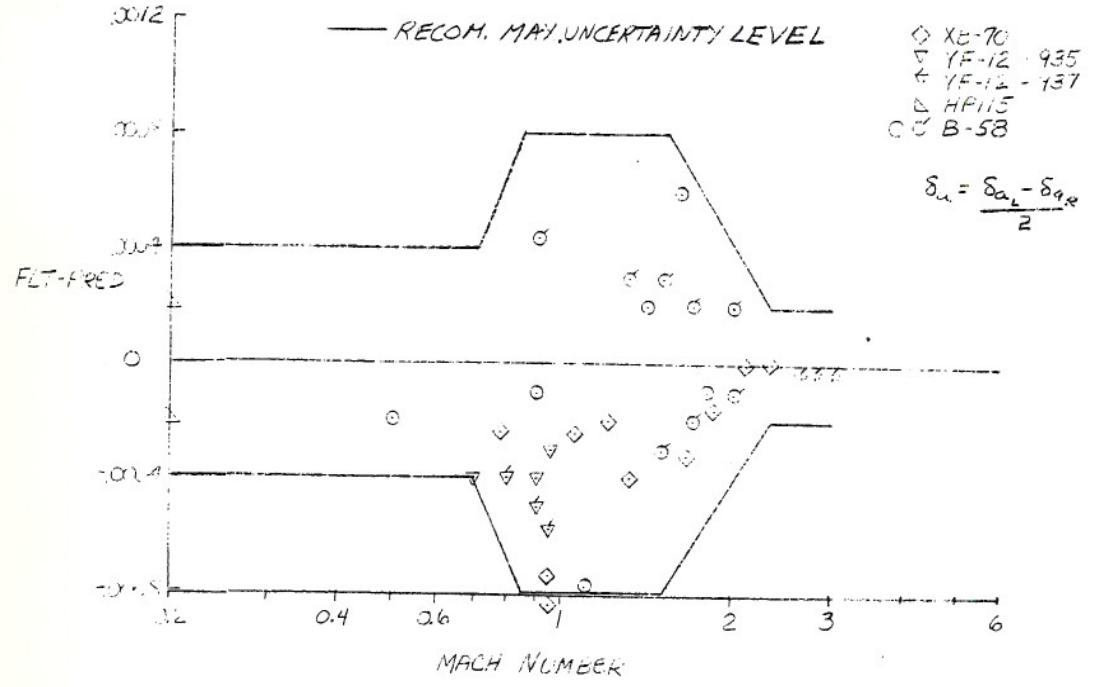

Figure 14. Correlation of flight and predicted $C_{n_{\delta_a}}$. Conventional aircraft.

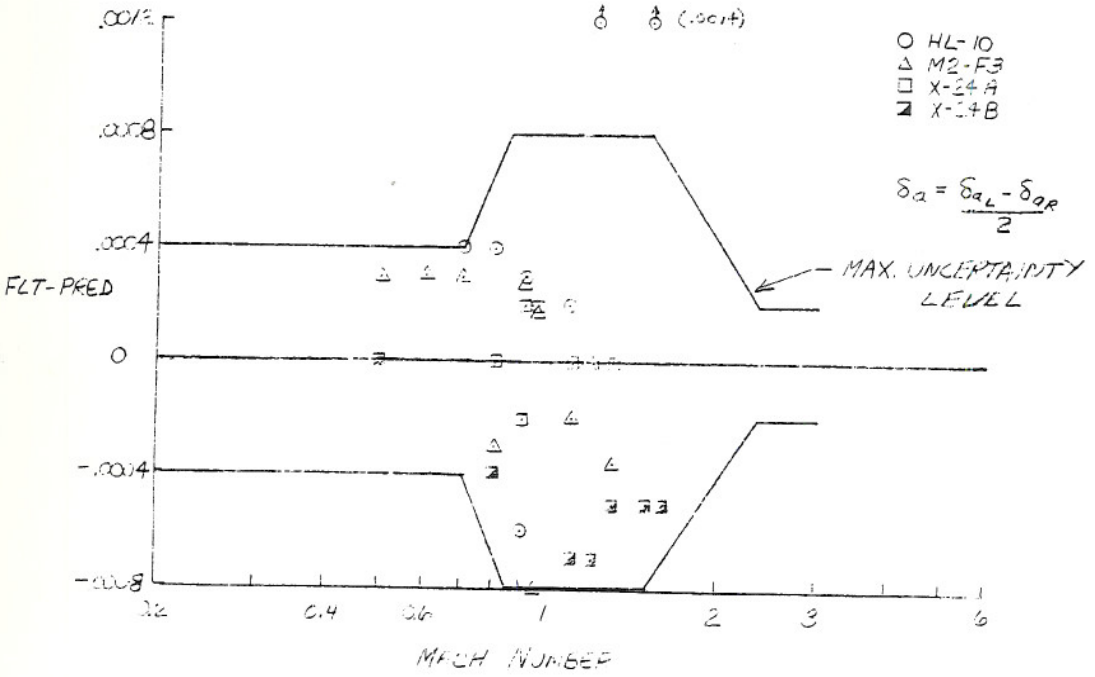

Figure 15. Correlation of flight and predicted $C_{n_{\delta_a}}$. Lifting bodies.

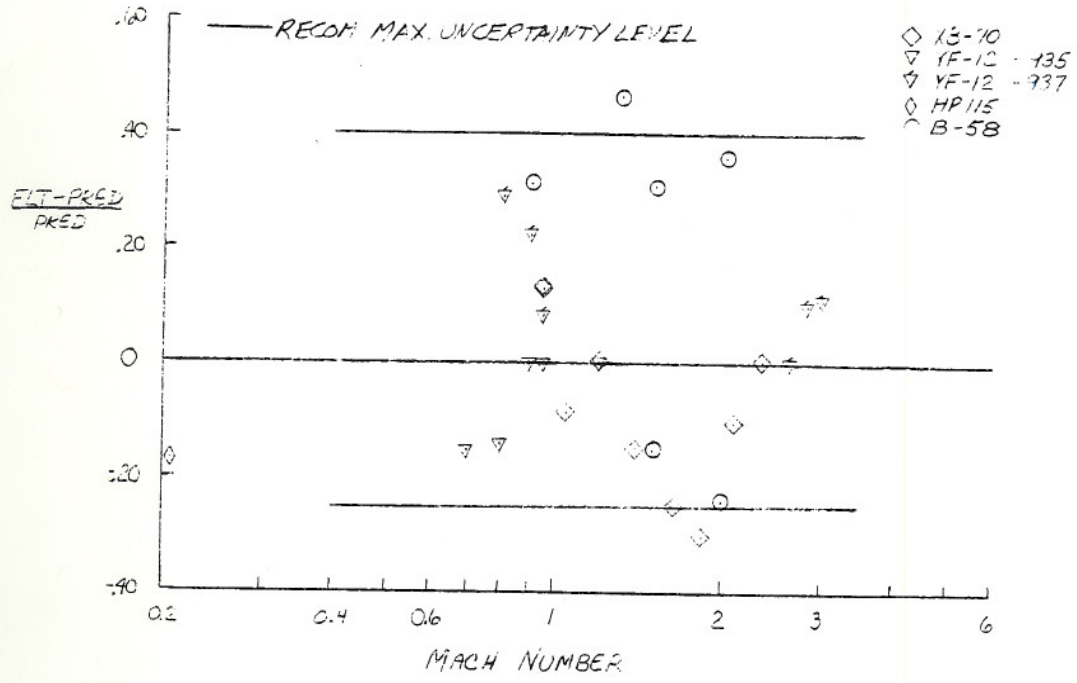

Figure 16. Correlation of flight and predicted $C_{\ell_{\delta_a}}$. Conventional aircraft.

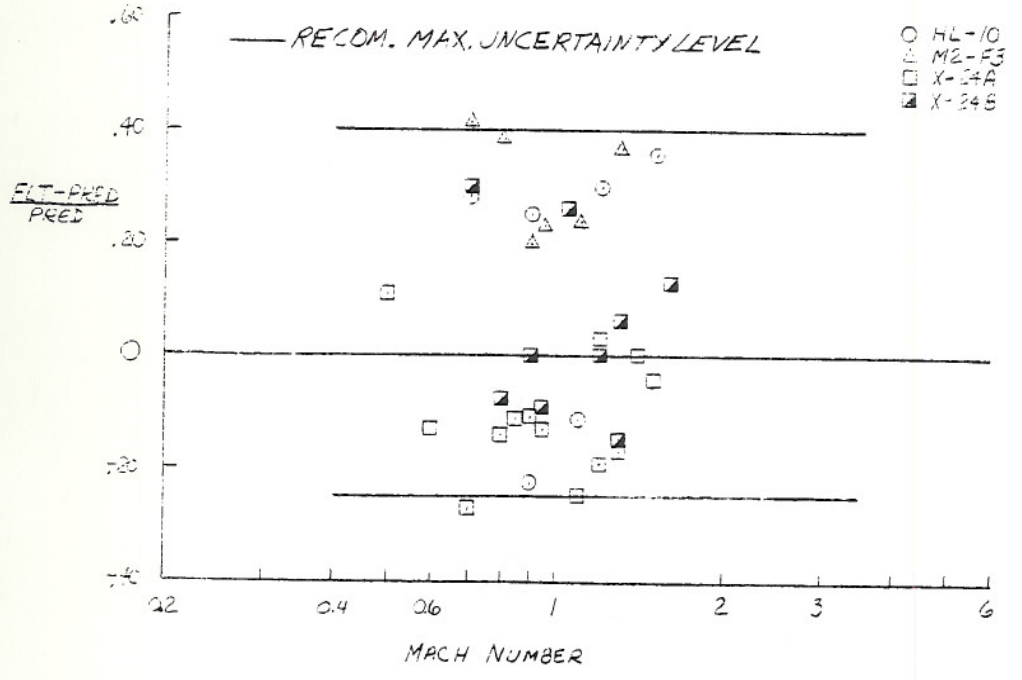

Figure 17. Correlation of flight and predicted $C_{\ell_{\delta_a}}$. Lifting bodies.

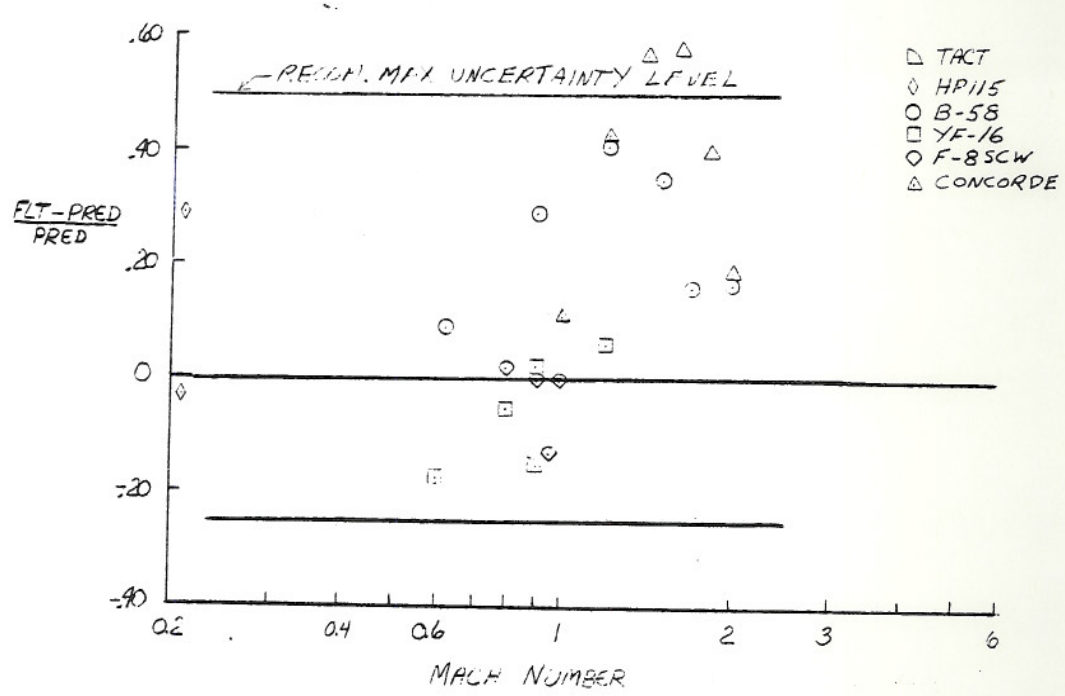

Figure 18. Correlation of flight and predicted $C_{n_{\delta_r}}$. Conventional aircraft.

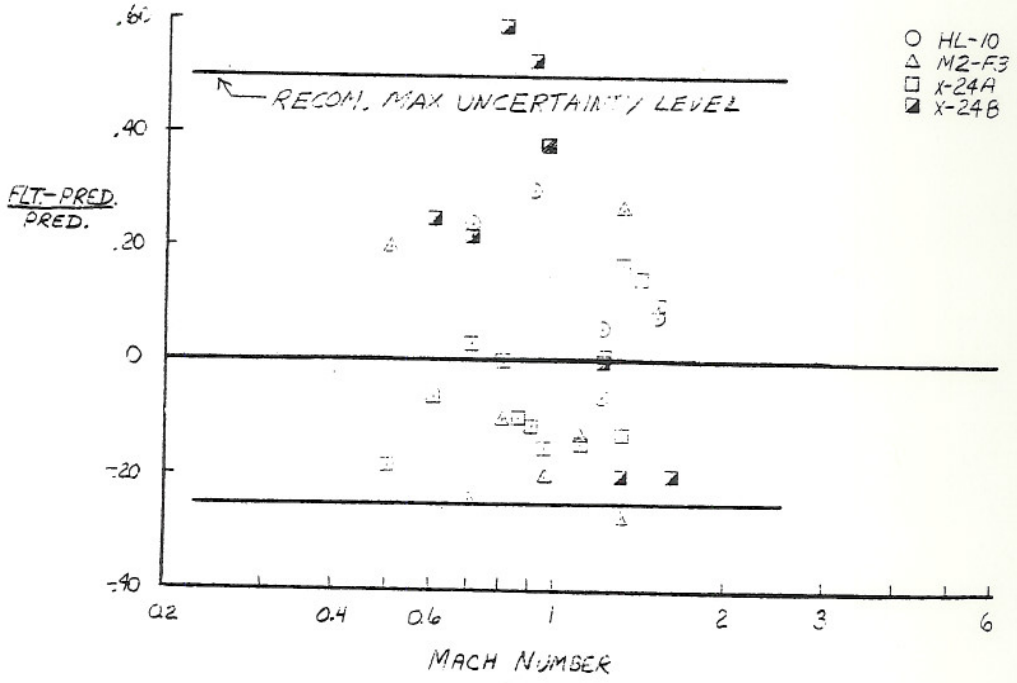

Figure 19. Correlation of flight and predicted $C_{n_{\delta_r}}$. Lifting bodies.

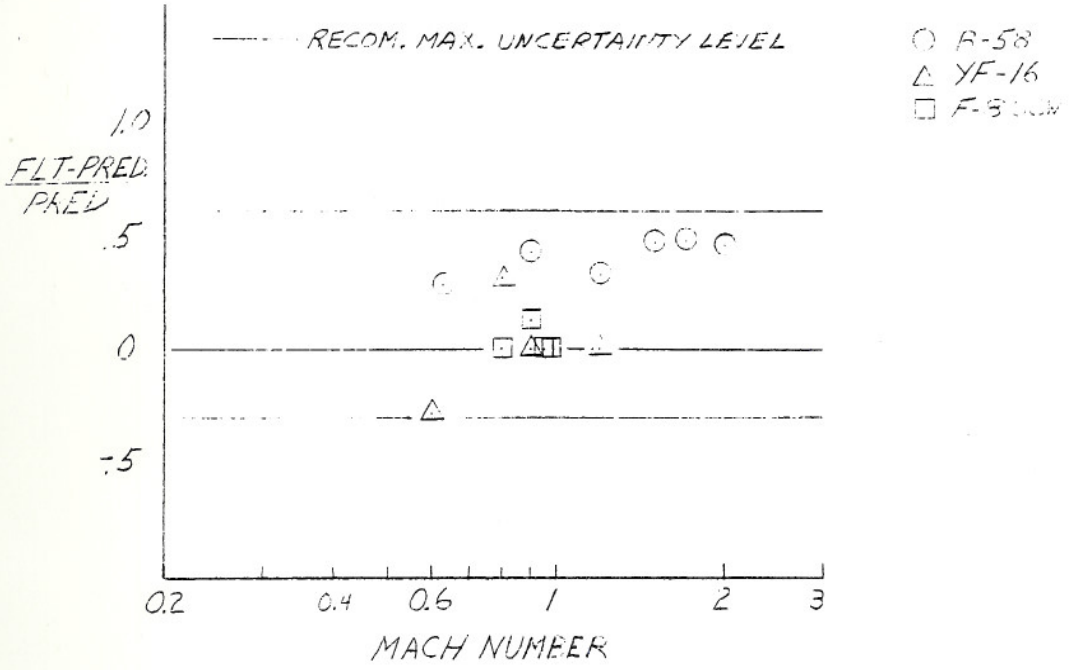

Figure 20. Correlation of flight and predicted $C_{\ell_{\delta_r}}$. Conventional aircraft.

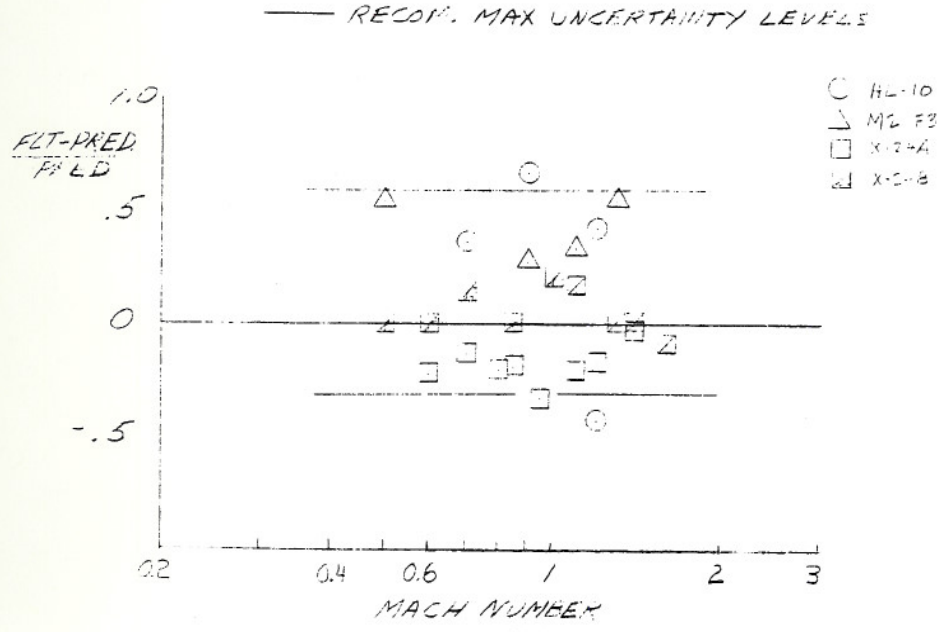

Figure 21. Correlation of flight and predicted $C_{\ell_{\delta_r}}$. Lifting bodies.

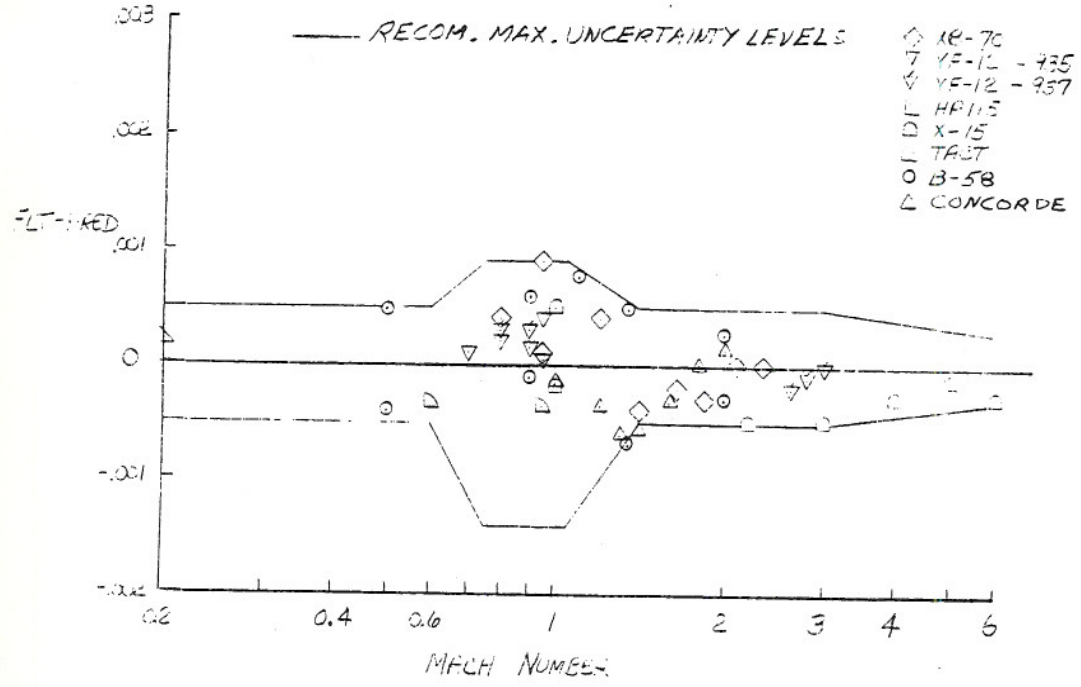

Figure 22. Correlation of flight and predicted C_{n_β}. Conventional aircraft.

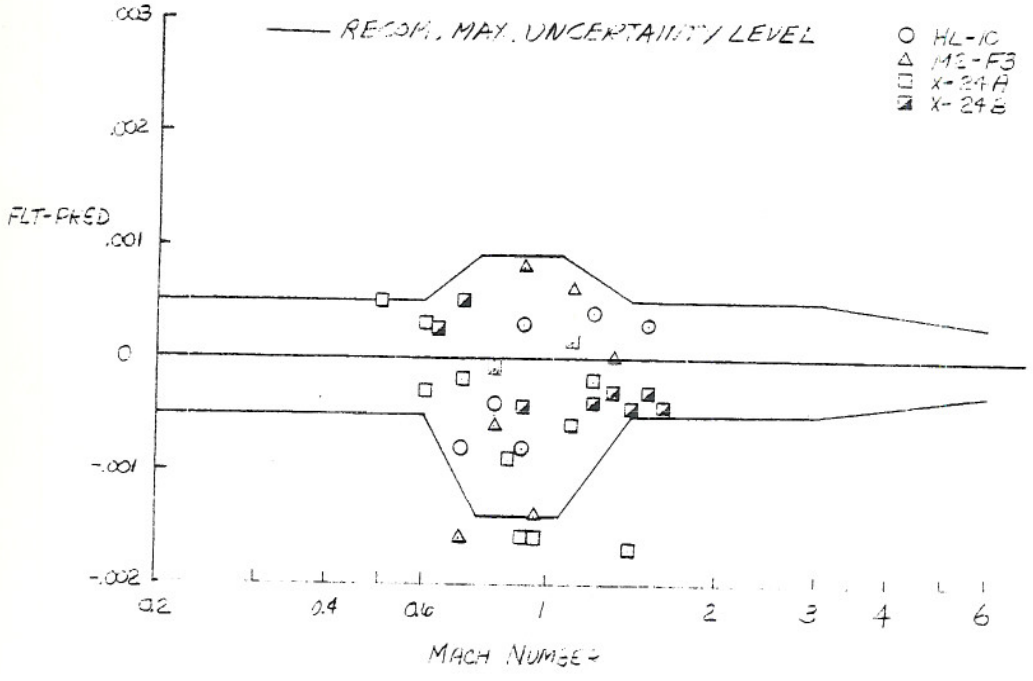

Figure 23. Correlation of flight and predicted C_{n_β}. Lifting bodies.

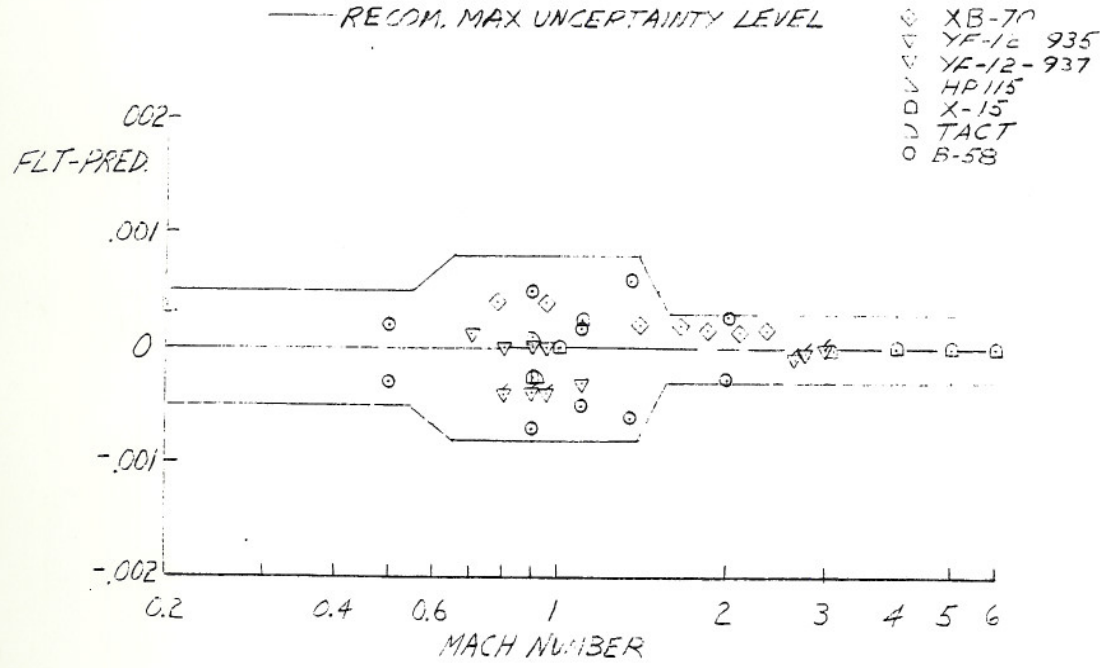

Figure 24. Correlation of flight and predicted C_{ℓ_β}. Conventional aircraft.

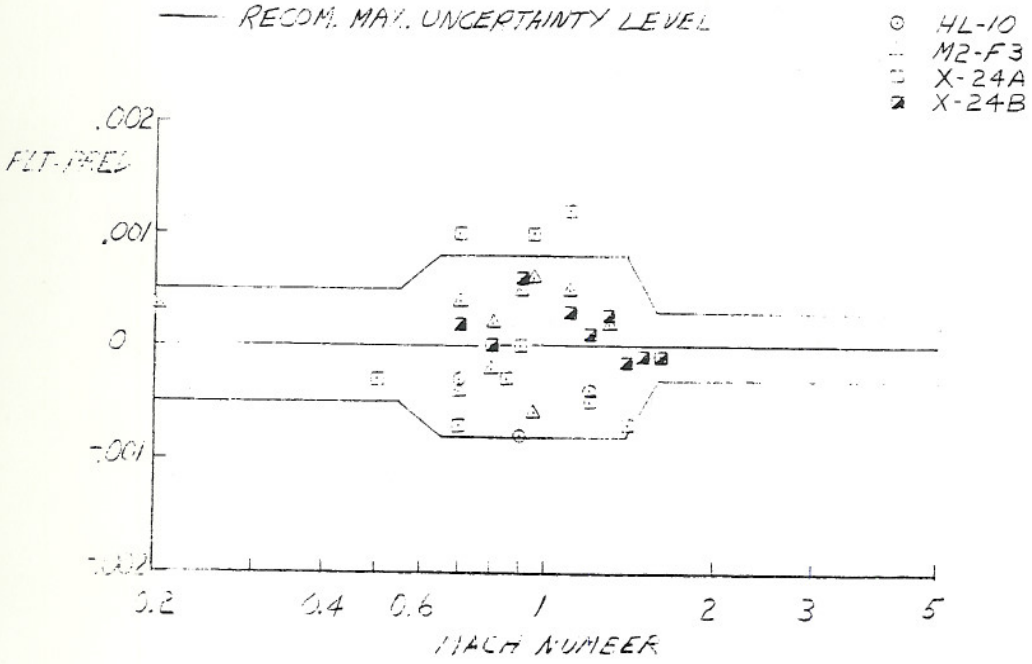

Figure 25. Correlation of flight and predicted C_{ℓ_β}. Lifting bodies.

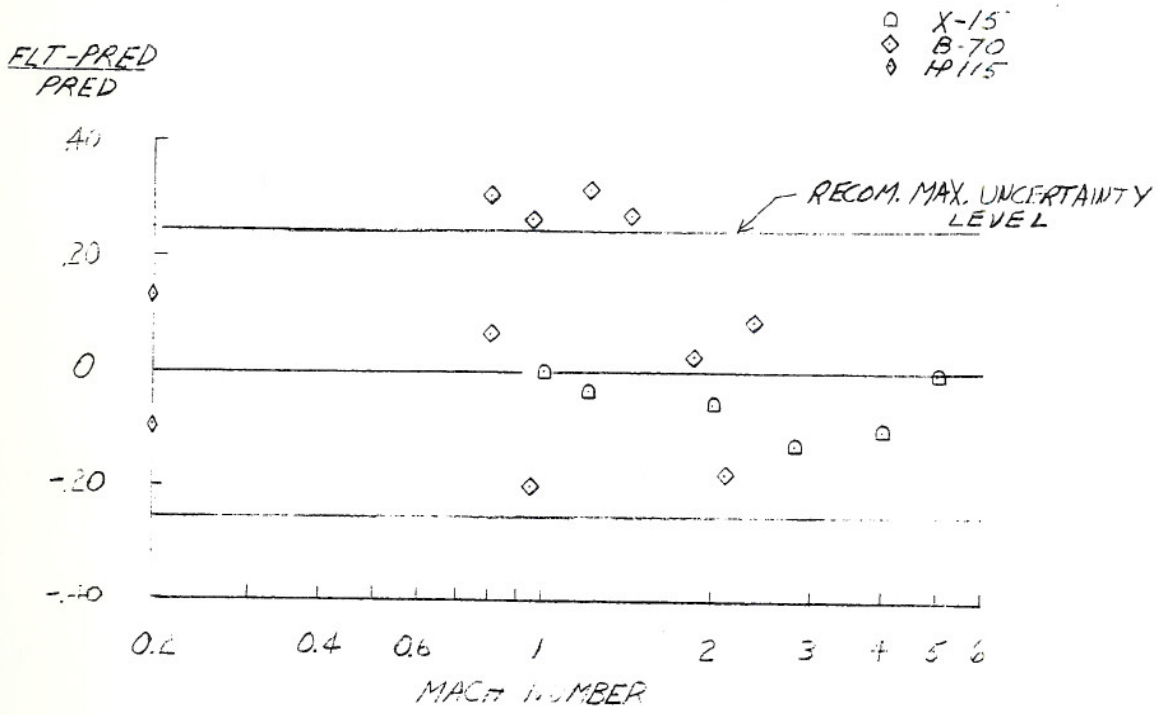

Figure 26. Correlation of flight and predicted C_{Y_β}. Conventional aircraft.

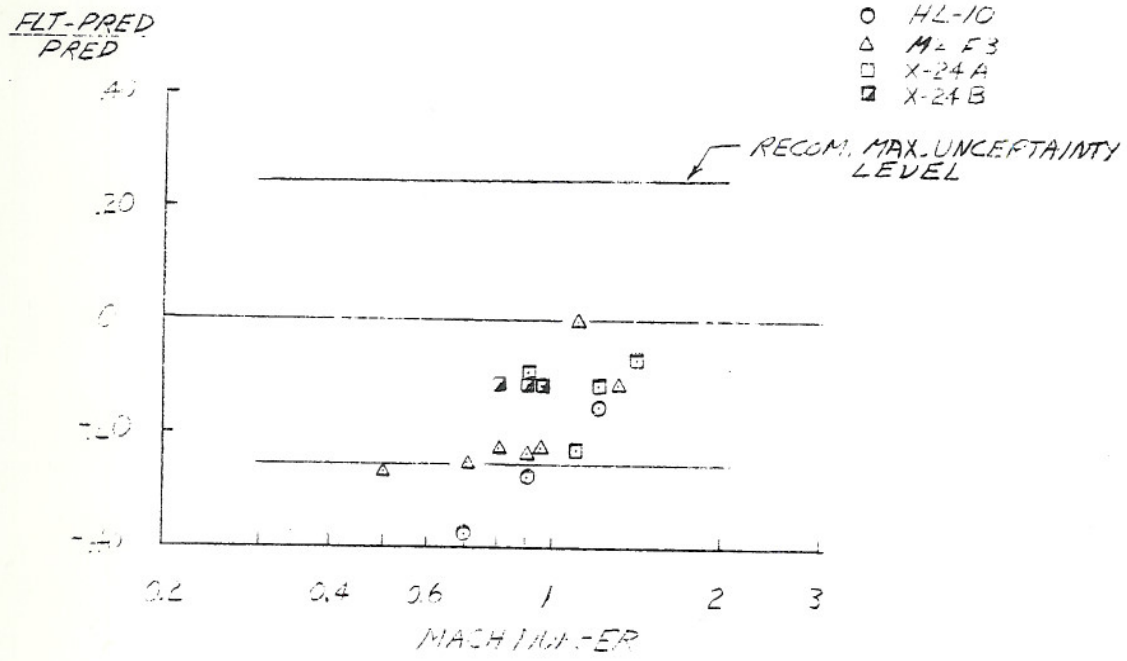

Figure 27. Correlation of flight and predicted C_{Y_β}. Lifting bodies.

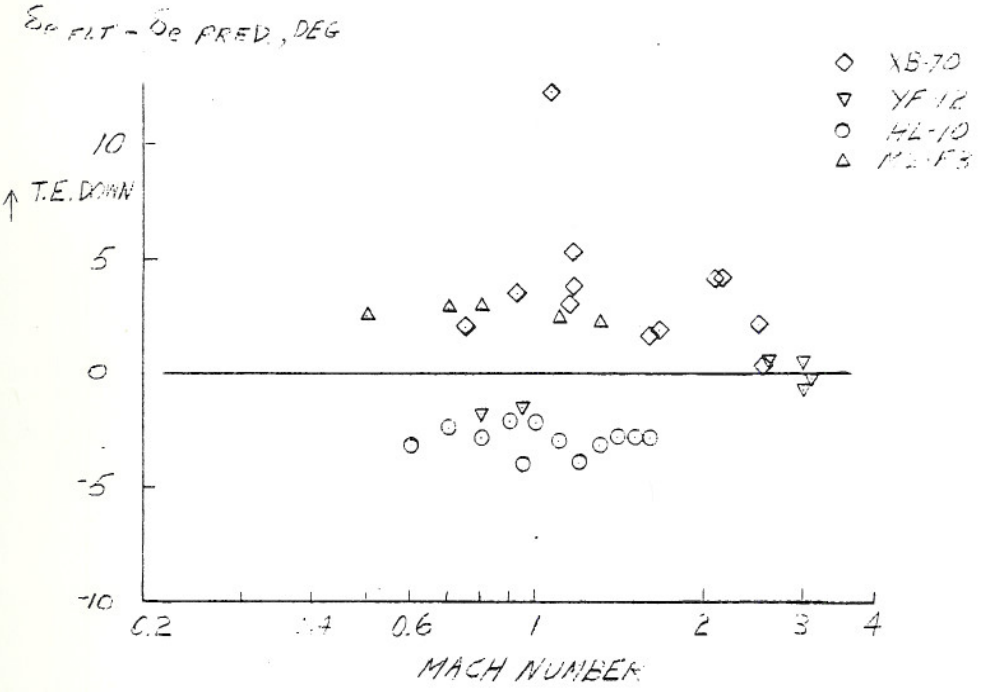

Figure 28. Correlation of flight and predicted trim δ_e.

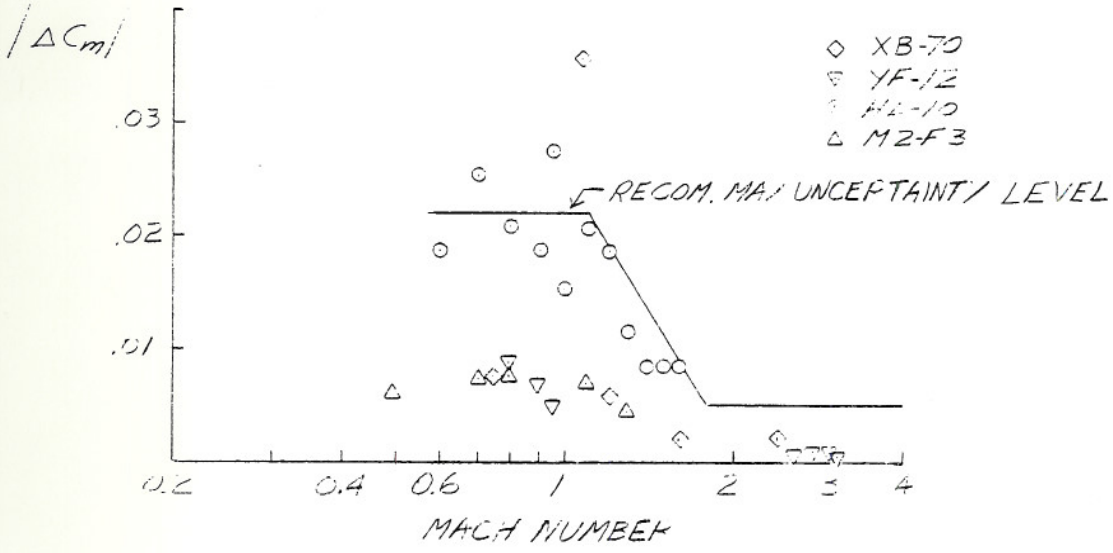

Figure 29. Correlation of flight and predicted ΔC_m.

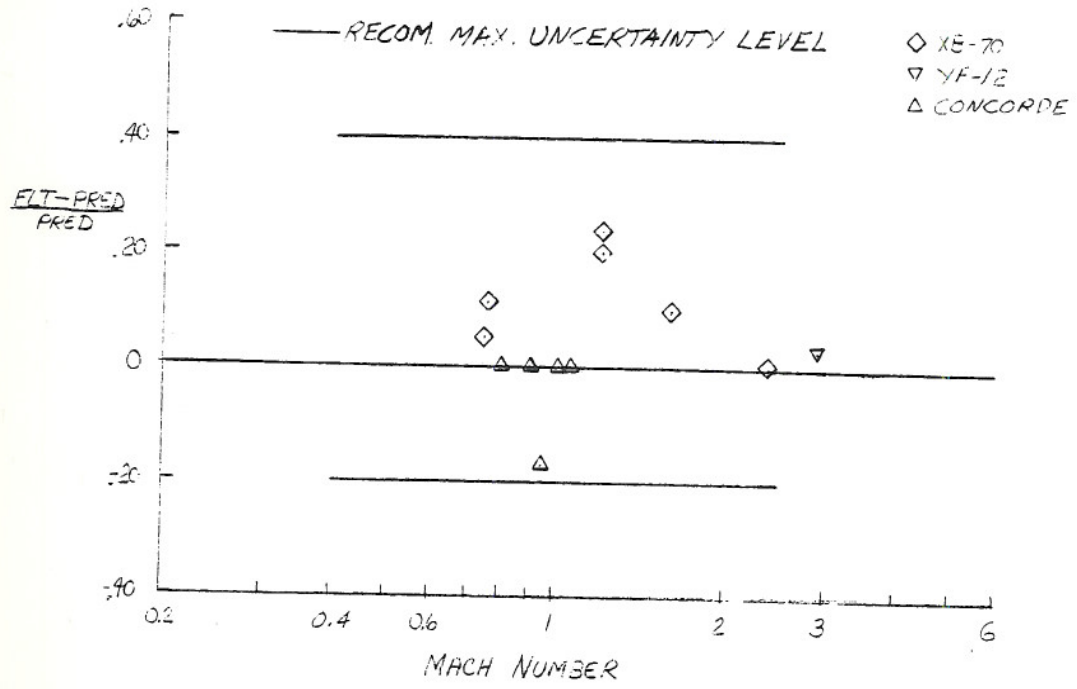

Figure 30. Correlation of flight and predicted $C_{m_{\delta_e}}$. Conventional aircraft.

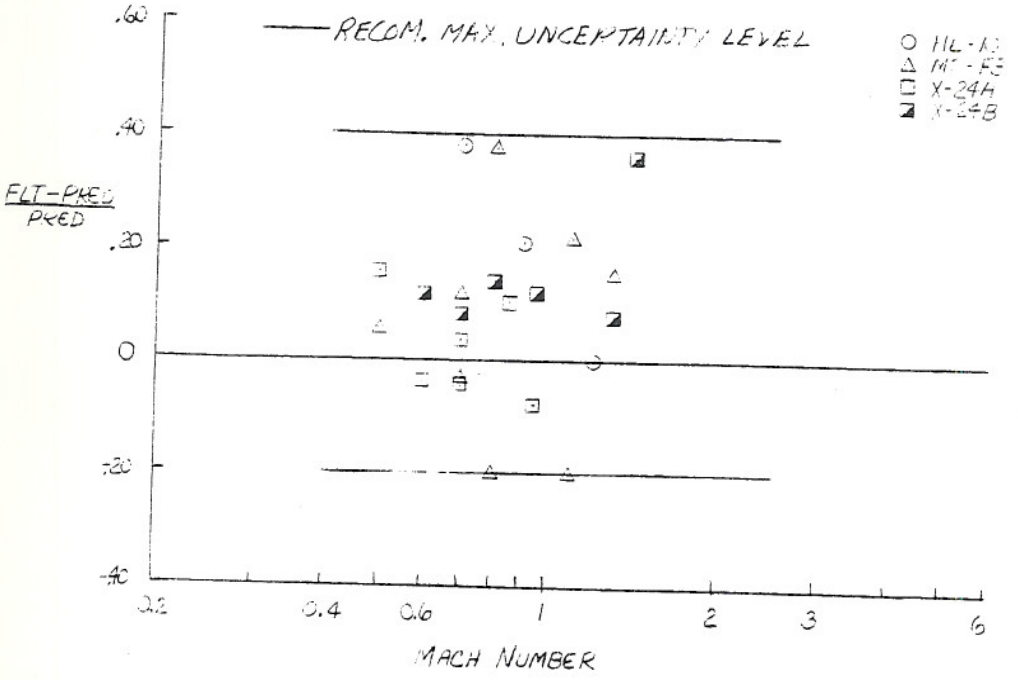

Figure 31. Correlation of flight and predicted $C_{m_{\delta_e}}$. Lifting bodies.

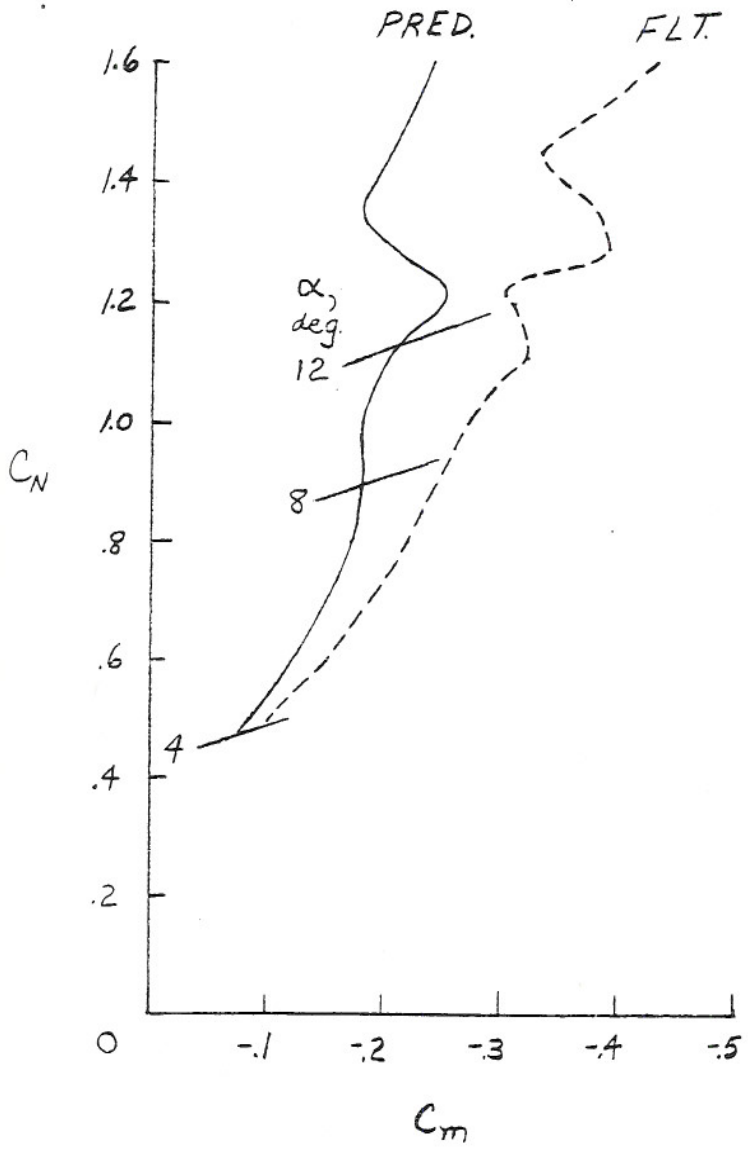

Figure 32. Illustration of nonlinear C_m characteristics.

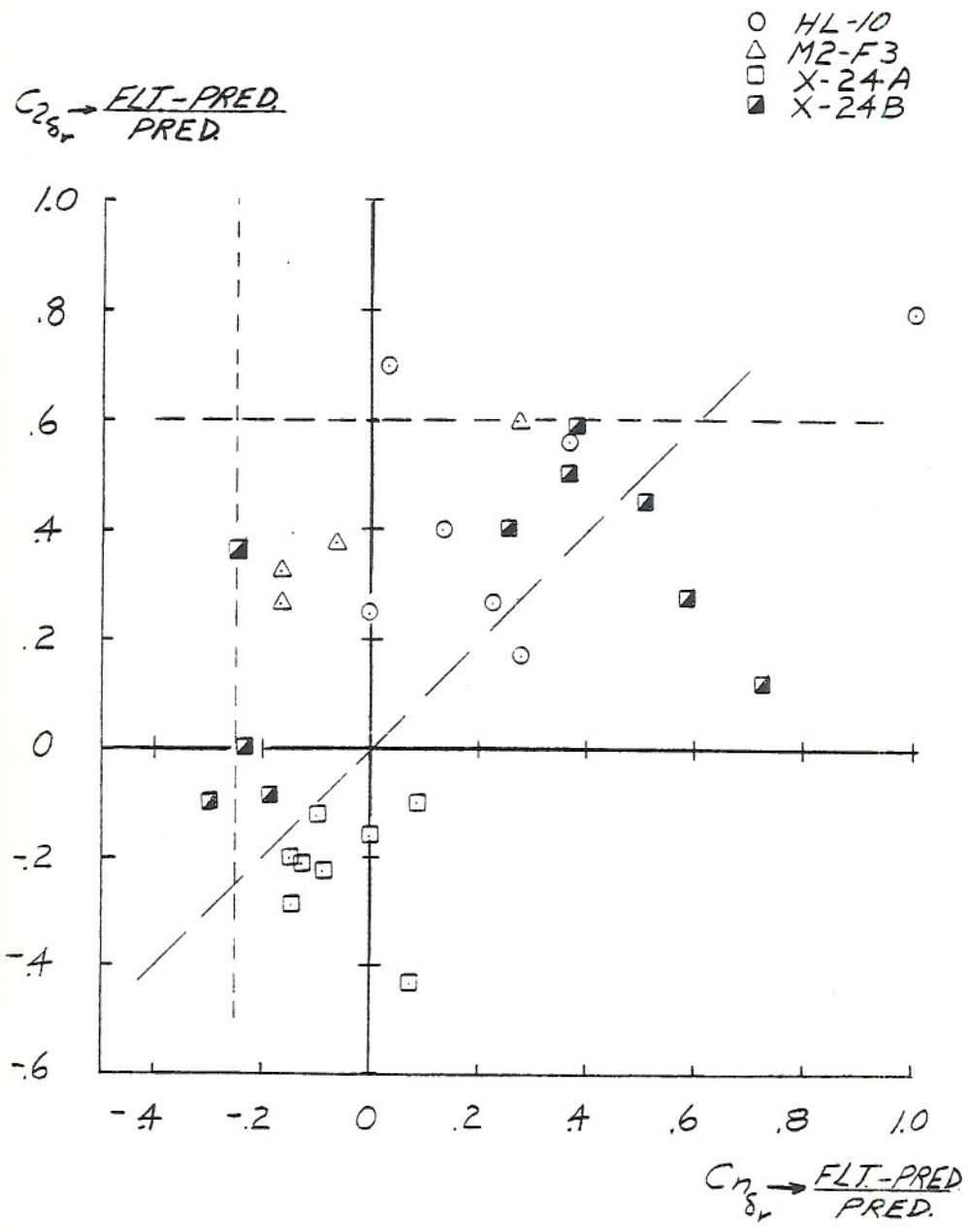

Figure 33. Relation of $C_{n_{\delta_r}}$ and $C_{\ell_{\delta_r}}$ uncertainties. Lifting bodies.

	M = 0.4		M = 0.6	
	ORBITER (TAILCONE OFF)	VARIATION CRITERIA	ORBITER (TAILCONE OFF)	VARIATION CRITERIA
ΔC_{n_β}	0.00015	$\pm$0.0005	0.00012	$\pm$0.0005
ΔC_{ℓ_β}	0.0004	$\pm$0.0005	0.0003	$\pm$0.00065
ΔC_{Y_β} RATIO*	-0.15	$\pm$0.25	-0.13	$\pm$0.25
$\Delta C_{\ell_{\delta_a}}$ RATIO	-0.10	-0.25	-0.05	-0.25
$\Delta C_{\ell_{\delta_r}}$ RATIO	-0.06	-0.30	-0.16	-0.30
$\Delta C_{n_{\delta_a}}$	0	$\pm$0.0004	-0.00015	$\pm$0.0004
$\Delta C_{n_{\delta_r}}$ RATIO	-0.17	-0.25	-0.16	-0.25
$\Delta C_{m_{\delta_e}}$ RATIO	-0.05	+0.40 -0.20	0	-0.20
$\Delta C_{m_{TRIM}}$	0.008	0.022	——	——

*ΔRATIO = $\frac{\text{FLT-PRED}}{\text{PRED}}$

Figure 34. Comparison of orbiter subsonic (ALT) derivative variations with DFRC maximum variation criteria.

1. Report No. NASA TM-81361	2. Government Accession No.	3. Recipient's Catalog No.
4. Title and Subtitle CORRELATION OF PREDICTED AND FLIGHT DERIVED STABILITY AND CONTROL DERIVATIVES - WITH PARTICULAR APPLICATION TO TAILLESS DELTA WING CONFIGURATIONS		5. Report Date 6. Performing Organization Code RTOP 989-10-00
7. Author(s) Joseph Weil and Bruce G. Powers		8. Performing Organization Report No. 10. Work Unit No.
9. Performing Organization Name and Address NASA Dryden Flight Research Center P.O. Box 273 Edwards, California 93523		11. Contract or Grant No. 13. Type of Report and Period Covered Technical Memorandum
12. Sponsoring Agency Name and Address National Aeronautics and Space Administration Washington, D.C. 20546		14. Sponsoring Agency Code

15. Supplementary Notes

16. Abstract

Flight derived longitudinal and lateral-directional stability and control derivatives were compared to wind-tunnel derived values. As a result of these comparisons, boundaries representing the uncertainties that could be expected from wind-tunnel predictions were established. These boundaries provide a useful guide for control system sensitivity studies prior to flight. The primary application for this data was the space shuttle, and as a result the configurations included in this study were those most applicable to the space shuttle. The configurations included conventional delta wing aircraft as well as the X-15 and lifting body vehicles.

17. Key Words (Suggested by Author(s)) Stability and control derivatives Wind-tunnel/flight comparison	18. Distribution Statement Unclassified—Unlimited STAR category 08

19. Security Classif. (of this report) Unclassified	20. Security Classif. (of this page) Unclassified	21. No. of Pages 43	22. Price* A03

*For sale by the National Technical Information Service, Springfield, Virginia 22161